RESEARCH ARTICLE

Variable influence of photosynthetic thermal acclimation on future carbon uptake in Australian wooded ecosystems under climate change

Alison C. Bennett[1,2] | Jürgen Knauer[3,4] | Lauren T. Bennett[5] |
Vanessa Haverd[3,†] | Stefan K. Arndt[1]

[1]School of Agriculture, Food and Ecosystem Sciences, University of Melbourne, Richmond, Victoria, Australia

[2]CSIRO, Environment, Aspendale, Victoria, Australia

[3]CSIRO, Oceans and Atmosphere, Canberra, Australian Capital Territory, Australia

[4]Hawkesbury Institute for the Environment, Western Sydney University, Richmond, New South Wales, Australia

[5]School of Agriculture, Food and Ecosystem Sciences, University of Melbourne, Creswick, Victoria, Australia

Correspondence
Alison C. Bennett, CSIRO, Environment, Aspendale, VIC, Australia.
Email: alison.bennett@csiro.au

Funding information
Australian Government Research Training Program

Abstract

Climate change will impact gross primary productivity (GPP), net primary productivity (NPP), and carbon storage in wooded ecosystems. The extent of change will be influenced by thermal acclimation of photosynthesis—the ability of plants to adjust net photosynthetic rates in response to growth temperatures—yet regional differences in acclimation effects among wooded ecosystems is currently unknown. We examined the effects of changing climate on 17 Australian wooded ecosystems with and without the effects of thermal acclimation of C3 photosynthesis. Ecosystems were drawn from five ecoregions (tropical savanna, tropical forest, Mediterranean woodlands, temperate woodlands, and temperate forests) that span Australia's climatic range. We used the CABLE-POP land surface model adapted with thermal acclimation functions and forced with HadGEM2-ES climate projections from RCP8.5. For each site and ecoregion we examined (a) effects of climate change on GPP, NPP, and live tree carbon storage; and (b) impacts of thermal acclimation of photosynthesis on simulated changes. Between the end of the historical (1976–2005) and projected (2070–2099) periods simulated annual carbon uptake increased in the majority of ecosystems by 26.1%–63.3% for GPP and 15%–61.5% for NPP. Thermal acclimation of photosynthesis further increased GPP and NPP in tropical savannas by 27.2% and 22.4% and by 11% and 10.1% in tropical forests with positive effects concentrated in the wet season (tropical savannas) and the warmer months (tropical forests). We predicted minimal effects of thermal acclimation of photosynthesis on GPP, NPP, and carbon storage in Mediterranean woodlands, temperate woodlands, and temperate forests. Overall, positive effects were strongly enhanced by increasing CO_2 concentrations under RCP8.5. We conclude that the direct effects of climate change will enhance carbon uptake and storage in Australian wooded ecosystems (likely due to CO_2 enrichment) and that benefits of thermal acclimation of photosynthesis will be restricted to tropical ecoregions.

KEYWORDS
carbon storage, carbon uptake, climate change, CO_2 enrichment, forest, gross primary productivity, net primary productivity, photosynthesis, thermal acclimation, vegetation carbon

[†]Vanessa Haverd passed away in January 2021 during early stages of model configuration. Her significant contribution to this work is vouched for by the first author.

1 | INTRODUCTION

Climate change poses an enormous threat to the potential productivity of wooded ecosystems. This is critical to the global carbon cycle because wooded ecosystems contribute 37 to 60 Pg C year^{-1} (~40%–50%) to global gross primary productivity (GPP; Cai et al., 2014) and store 300 to 363 Pg C in live biomass (Kohl et al., 2015; Pan et al., 2011). Since the end of the 19th century global average surface temperatures have increased by around 1.1°C with the most extreme emissions scenario projecting further increases of up to 3.3°C by 2100 (i.e., total increase of 4.4°C under SSP5-8.5, IPCC, 2021). Under this scenario (SSP5-8.5) average air temperatures may exceed current conditions by a minimum of 3°C in tropical regions and a maximum of 8°C in arctic/boreal regions by 2100 (Arias et al., 2021). Such large temperature increases could push wooded ecosystems into thermal regimes that are suboptimal for carbon uptake if average air temperatures exceed current thermal optima for GPP (T_{opt}, Huang et al., 2019). This would have significant impacts on GPP with potential flow-on effects to net primary productivity (NPP) and vegetation carbon storage. However, since plants have the capacity to adjust photosynthesis to growth temperature (Yamori et al., 2014), many wooded ecosystems may adjust (i.e., acclimate) GPP as their temperature regimes change. The extent to which this adjustment will alter the future carbon uptake and storage of wooded ecosystems at regional scales remains largely unexamined.

Acclimation of photosynthesis to growth temperature in C$_3$ plants, the dominant photosynthetic pathway in woody ecosystems, has been firmly established by many experimental studies (see e.g. Aspinwall et al., 2016; Bermudez et al., 2021; Gunderson et al., 2010; Mooney et al., 1978; Scafaro et al., 2017; Sendall et al., 2015; Slot & Winter, 2017). Whilst not all plants have shown acclimation (Dillaway & Kruger, 2010; Drake et al., 2016; Smith et al., 2020), for those that do, the type and strength of acclimation response can vary with species (Dusenge et al., 2019; Gunderson et al., 2010; Li et al., 2016), plant functional type (PFT; Smith & Dukes, 2017; Way & Yamori, 2014; Yamori et al., 2014), climate of origin (Drake et al., 2015), and season (Kolari et al., 2014; Lin et al., 2013). Plants that acclimate use various mechanisms. For example, plants grown at reduced temperature can increase the quantity of photosynthetic enzymes and/or the ratio of unsaturated to saturated fatty acids, whilst plants grown at increased temperature can increase membrane integrity and electron transport capacity, decrease the activation state of Rubisco, alter the expression of heat shock proteins, and/or decrease the ratio of unsaturated to saturated fatty acids (Yamori et al., 2014). Through these adjustments, plants can thus photosynthesize more effectively at their growing temperature within as little as 1–14 days (Vico et al., 2019). This acclimation to air temperature may impart a strong effect on ecosystem-scale photosynthesis (i.e., GPP), carbon gain (as NPP), and the accumulation of carbon in terrestrial pools (i.e., biomass, litter, and soil carbon pools) as the climate warms.

The ability of plants to acclimate photosynthesis to growth temperature has the potential to significantly influence model predictions of ecosystem carbon dynamics under climate change (Arneth et al., 2012; Booth et al., 2012; Smith & Dukes, 2013). Under the most extreme emissions scenario, including thermal acclimation of photosynthesis in global-scale simulations increased average photosynthetic rates (Smith et al., 2017) and terrestrial carbon storage (Lombardozzi et al., 2015; Mercado et al., 2018; Smith et al., 2016) by the end of the 21st century relative to simulations without thermal acclimation of photosynthesis. Annual average net photosynthetic rates were predicted to increase by 56.8 g C m^{-2} year^{-1} in simulations using the Community Earth System Model (Smith et al., 2017), whereas total global land carbon storage was predicted to increase by 8 ± 6% (35 ± 14 Pg C) using the Joint UK Land Environment Simulator (JULES; Mercado et al., 2018) and by ~10% (10.7 ± 1.1 Pg C) using Community Land Model (CLM; Lombardozzi et al., 2015). When thermal acclimation of foliar respiration was also included land carbon storage was higher by ~6% at the end of the century using Land Model 3 (LM3; Smith et al., 2016) and by 22% in CLM (Lombardozzi et al., 2015).

Despite indications from global-scale simulations, questions remain regarding regional variations in the influence of photosynthetic thermal acclimation on carbon uptake and storage. In the tropics, including thermal acclimation enhanced photosynthesis by ~190 g C m^2 year^{-1} (Smith et al., 2017) and average GPP by ~30% (Mercado et al., 2018). However, predicted outcomes with thermal acclimation for tropical carbon storage range from decreased vegetation carbon (Smith et al., 2016, noting that foliar respiratory acclimation was also included), to minor increases in ecosystem carbon storage (Lombardozzi et al., 2015), to increased land carbon storage by ~9.6 ± 5.8% (Mercado et al., 2018). Likewise, in arctic/boreal regions thermal acclimation of photosynthesis was alternately predicted to increase photosynthesis by ~95 g C m^2 year^{-1} (Smith et al., 2017) and to increase land carbon gains (Lombardozzi et al., 2015) or to decrease land carbon by ~3.5% (Mercado et al., 2018). Overall, model simulations demonstrate a substantial effect of thermal acclimation of photosynthesis on future GPP and carbon storage at the global scale, however there are significant geographic differences in the direction of the effect. Though alternate model implementations may explain those differences, they also indicate scope for examining the contrasting impacts on wooded ecosystems at regional to continental scales.

Despite the importance of wooded ecosystems to land carbon storage, very little research has directly examined the effects of thermal acclimation of photosynthesis on simulated productivity (i.e., GPP and NPP) and subsequent carbon storage at sub-global scales. To our knowledge, only two simulation studies have examined effects of thermal acclimation of photosynthesis on woody productivity at regional scales. Chen and Zhuang (2013) simulated forest carbon dynamics using Terrestrial Ecosystem Model (TEM) across Northern America to 2100 under four scenarios that ranged from high (A1F1) to low (B2) emissions. They demonstrated that thermal acclimation of photosynthesis increased GPP, NPP, net ecosystem productivity (NEP), and carbon storage relative to simulations that excluded thermal acclimation of photosynthesis

with the greatest effect under the high emissions scenario where GPP was predicted to increase by 0.53 Pg C year^{-1} and vegetation carbon by 7.25 Pg C. Furthermore, increases varied by location across North America with a greater effect in the south than the north and west that was likely caused by climatic differences. In the second study, Stinziano et al. (2019) examined effects of photosynthetic thermal acclimation on net carbon gain of a single Canadian boreal tree species to 2100 using the MAESTRA stand-level model. In their simulations, carbon gain increased by as much as 175% or decreased by 1%–2% with the effect entirely dependent upon the choice of parameters that were acclimated. Neither study examined the effects of photosynthetic thermal acclimation on modelled productivity and carbon storage at the ecosystem-scale, leaving a substantial knowledge gap in our understanding of these effects at the scales between species and region.

Novel functions for incorporating thermal acclimation of photosynthesis within land surface models (LSMs) became available in 2019 (Kumarathunge et al., 2019). These functions extend on earlier work of Kattge and Knorr (2007) by expanding the temperature domain from 18–35°C (Kattge & Knorr, 2007) to 3–37°C; incorporating a broader array of PFTs (six as opposed to three); and separately incorporating acclimation to growth temperature (i.e., mean air temperature of preceding 30 days) and adaptation to temperature of origin (i.e., 30-year mean maximum temperature of the warmest month). These improvements broaden the functions' application in LSMs and more accurately represent the temperature responses of Vc_{max} and J_{max} compared with Kattge and Knorr (2007) according to Smith and Keenan (2020). Despite these improvements, we are unaware of any studies that have incorporated these novel functions in LSMs (except for Knauer et al., 2023 who used the implementation we report herein to conduct global-scale simulations), and until now they have not been used to model future carbon uptake and storage at regional scales.

Australian wooded ecosystems are ideal for examining the effects of photosynthetic thermal acclimation on carbon uptake and storage under climate change at the ecosystem scale. Wooded ecosystems within the continent occur across a broad thermal range (mean annual temperature [MAT] 4.4–29.1°C) encompassing tropical, subtropical and temperate climate zones (Bennett et al., 2020). Additionally, the OzFlux network of eddy covariance flux towers has been continuously measuring ecosystem fluxes in wooded ecosystems in five ecoregions (Beringer et al., 2016, 2022) providing a rich source of CO_2 exchange data. Furthermore, recent evidence suggests that GPP across 17 of these ecosystems has adjusted to the local temperature regime indicating that GPP is thermally adjusted to the environment (Bennett et al., 2021). Together, these factors enable site-level optimization of parameters within a land-surface model so that GPP, NPP, and vegetation carbon storage may be simulated under future climatic regimes across a suite of wooded ecosystems from diverse thermal regimes. While boreal climates and deciduous forests are not represented, Australia's wooded ecosystems can be used to illuminate the effects of thermal acclimation

of photosynthesis on the GPP, NPP, and live tree carbon storage in evergreen ecosystems across all seasons.

Our study examined the extent to which thermal acclimation of photosynthesis affects simulated GPP, NPP, and live tree carbon storage in 17 Australian wooded ecosystems from five ecoregions under climate change. We were interested in understanding differences in the direct effects of climate change (i.e., increasing temperature, elevated CO_2, and changing precipitation) among ecoregions and whether there were regional differences in the effect of thermal acclimation of photosynthesis. Our research questions were (1) How will future GPP, NPP, and live tree carbon storage in Australia's wooded ecosystems change with an extreme scenario of climate change? (2) What is the impact of thermal acclimation of photosynthesis on projected changes in GPP, NPP, and live tree carbon storage?

2 | MATERIALS AND METHODS

2.1 | Study sites

We selected 17 wooded ecosystems from the Australian TERN OzFlux network of micro-meteorological flux stations (Figure 1; Beringer et al., 2016). Study sites spanned the Australian continent, covering a broad range in latitude (−12.5° to −43.10°), longitude (115.71° to 150.72°), MAT (9.7°C ± 0.65 to 27.1°C ± 0.99, SD), and mean annual precipitation (MAP; 265 mm ± 108 to 4239 mm ± 1461, SD; Bennett et al., 2021). The sites represent five ecoregions (tropical forests, tropical savannas, Mediterranean woodlands, temperate woodlands, and temperate forests; Department of Agriculture Water and the Environment, 2018) and four major climate zones (Tropical, Subtropical, Grassland, and Temperate) of the modified Köppen climate classes for Australia; (Bureau of Meteorology, 2020). Sites were selected on the basis that (a) the vegetation was dominated by woody tree species; (b) more than 1 year of continuously recorded eddy covariance flux data were available for site-level parameter optimization; and (c) the vegetation was in a minimally disturbed natural state during the eddy covariance measurement period (i.e., no history of severe fires, intensive management, or agriculture within 10 years).

2.2 | CABLE-POP model description

We used the Community Atmosphere Biosphere Land Exchange model (CABLE-POP) developed by Australia's Commonwealth Scientific and Industrial Research Organisation (CSIRO; Haverd et al., 2018). CABLE-POP is a two-leaf (sunlit and shaded) LSM that contributes to the Global Carbon Budget (Friedlingstein et al., 2022). It simulates ecosystem processes through four coupled modules: a biophysics core (CABLE, Wang & Leuning, 1998); a biogeochemistry module (CASA-CNP, Wang et al., 2010), the Population Orders Physiology module (POP) for woody demography
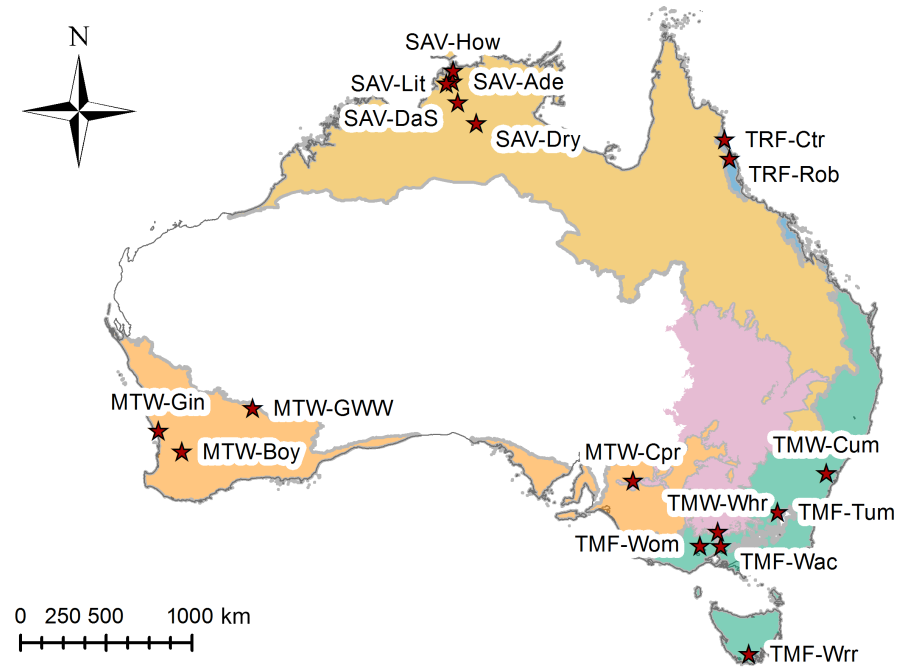
FIGURE 1 Location of the 17 study sites showing their abbreviated global ecoregion name from the Interim Biogeographic Regionalisation for Australia v7 (Department of Agriculture Water and the Environment, 2018). The full ecoregion names are provided in Table S1. The site labels are the three-letter prefix of site ecoregion and three-letter suffix of the OzFlux site name. Map lines delineate study areas and do not necessarily depict accepted national boundaries.

Ecoregion
- Tropical savannas (SAV)
- Tropical forests (TRF)
- Mediterranean woodlands (MTW)
- Temperate woodlands (TMW)
- Temperate forests (TMF)

★ Study site

(Haverd et al., 2014; Haverd, Smith, et al., 2013), and the POPLUC land use and land cover change module (Haverd et al., 2018), although POPLUC was disabled for this study. CABLE uses the Farquhar et al. (1980) model of photosynthesis to simulate half-hourly GPP and then transfers daily sums of GPP to CASA-CNP, which calculates autotrophic respiration and allocates the remaining NPP to leaves, stems and fine roots. CASA-CNP also transfers carbon, nitrogen, and phosphorous between pools and thus simulates the effects of nutrient limitation on photosynthesis. CABLE simulates fluxes within two tiles, one grass and one forest, and then calculates the total ecosystem fluxes as the area-weighted tile average. The model also includes functions for the temperature acclimation of leaf, stem and root respiration as described by Atkin et al. (2015). The source code is available at https://trac.nci.org.au/trac/cable/branches/Users/ab7412/GPP_temp (Revisions 9625 and 9627).

We carefully configured CABLE-POP to optimize photosynthetic performance across our range of wooded sites. Leaf area index was calculated based on the pipe model of Shinozaki et al. (1964) as described by Haverd et al. (2018), which determines C allocation to leaves and stem based on a constant leaf to sapwood area on the basis that this improved model performance in Northern Hemisphere FACE studies (De Kauwe et al., 2014). The ratio of J_{max} to Vc_{max} ($J{:}V$), critical to climate sensitivity of photosynthesis, was dynamically adjusted to be co-limiting instead of assuming a fixed ratio ($J{:}V$) at a given temperature using functions derived from

co-ordination theory (Chen et al., 1993). "Co-ordination of photosynthesis" updates $J{:}V$ on a daily basis by redistributing total canopy nitrogen between Rubisco limited and electron-transport limited photosynthesis based on the leaf environment of the last 5 days (Haverd et al., 2018). Stomatal conductance was calculated following Medlyn et al. (2011).

2.3 | Thermal acclimation of photosynthesis in CABLE-POP

We integrated functions for the acclimation and adaptation of photosynthetic parameters developed by Kumarathunge et al. (2019) into the CABLE-POP code (Knauer et al., 2023). These functions adjust parameters of the peaked Arrhenius equation (Equation 1, Johnson et al., 1942) that describes the temperature dependence of J_{max} and Vc_{max} within the Farquhar et al. (1980) model of photosynthesis.

$$k_{T_k} = k_{25}\exp\left[\frac{E_a \times 10^3 (T_k - 298.15)}{298.15 R T_k}\right] \cdot \frac{1 + \exp\left(\frac{298.15 \Delta S - H_d}{298.15 R}\right)}{1 + \exp\left(1 + \exp\frac{T_k \Delta S - H_d}{(T_k R)}\right)},$$
(1)

where k_{T_k} is the process rate ($\mu mol\, m^{-2}\, s^{-1}$) of either J_{max} or Vc_{max} at leaf temperature T_k, k_{25} is the process rate at 25°C (calculated as a function of leaf N and leaf P following Walker et al., 2014), E_a is the activation

energy (kJ mol^{-1}), T_k is the leaf temperature (K), R is the universal gas constant (8.314 J mol^{-1} K^{-1}), ΔS is the entropy term (J mol^{-1} K^{-1}), and H_d is the deactivation energy set to 200,000 J mol^{-1} as described by Medlyn et al. (2002; Table S2). Specifically, the functions (Equations 2–4 below) adjust the activation energy of Vc_{max} (E_{aV}, kJ mol^{-1}) and the entropy terms for Vc_{max} (ΔS_V, J mol^{-1} K^{-1}), and J_{max} (ΔS_J, J mol^{-1} K^{-1}) as a function of the mean daily temperature of the preceding 31 days (T_{growth}) and the mean maximum temperature of the warmest month for the previous 20 years (T_{home}, Figure S1). Note that our implementation differs slightly from Kumarathunge et al. (2019), where T_{growth} is calculated on the previous 30 days, and T_{home} from the previous 30 years.

$$E_{av} = 42.6 + 1.14T_{growth}, \tag{2}$$

$$\Delta S_v = 645.13 - 0.38T_{growth}, \tag{3}$$

$$\Delta S_j = 658.77 - 0.84T_{home} - 0.52\left(T_{growth} - T_{home}\right). \tag{4}$$

The Kumarathunge et al. (2019) functions also acclimate $J{:}V$ (JV_r); however the model's "co-ordination of photosynthesis" functions (Haverd et al., 2018) overwrite this effect by updating $J{:}V$ on a daily basis. We selected these functions in preference to the more established Kattge and Knorr (2007) functions due to the wider thermal domain and broader array of represented species (141 vs. 36). This ensured relevance to Australian plant species, and that our simulations were within the functions' thermal domain under most conditions.

2.4 | Site parameter optimization

CABLE parameters were optimized using BeoPEST ver 14.02, the parallel implementation of "PEST" model-independent parameter estimation software (Doherty, 2017). PEST was run in parameter estimation mode, which uses the Gauss-Marquardt–Levenberg method to minimize the least-squares objective function of the difference between an observation and the model output for that observation. Parameters were optimized at the site level on the basis that photosynthetic parameters are more varied at the site than at the broader PFT-scale (Groenendijk et al., 2011) and that different parameter values within a PFT can significantly influence modelled relative photosynthetic responses to climate change (Stinziano et al., 2019). We optimized parameters of the forest tile only, for the evergreen broadleaved forest PFT for all sites. Eddy-covariance data from each of the 17 wooded sites were used to optimize four CABLE-POP parameters selected based on their effect on canopy-scale photosynthesis (Table 1; Figure 2). Half-hourly (or hourly, TMF-Tum) eddy covariance GPP and ET flux observations from each of the 17 study sites were downloaded from https://dap.ozflux.org.au/thredds/catalog.html and pre-processed as described in Bennett et al. (2021). From these data we calculated median monthly diurnal cycles of GPP and ET for (a) all observations (2 groups), (b) observations with Ta_max in the 10th percentile (i.e., low extreme, 2 groups), (c) observations with Ta_max in the 90th

percentile (i.e., high extreme, 2 groups), and (d) the boundary line relationship (at the 90th percentile) between GPP and Ta (1 group, Bennett et al., 2021). These seven observation groups were then used by PEST to optimize the four selected CABLE parameters for each site. We optimized "g1," the sensitivity of stomatal conductance to assimilation rate (Medlyn et al., 2011); "gamma," the sensitivity of roots and stomatal conductance to soil moisture (Haverd, Raupach, et al., 2013); "extkn," which affects the vertical distribution of leaf nitrogen through the canopy (Wang & Leuning, 1998); and "vcmax_sc," which scales the relationship between Vc_{max} and leaf Nitrogen (N) described by Walker et al. (2014). Optimization was constrained within upper and lower parameter values such that "g1" remained within the physiological limits presented by Lin et al. (2015), "gamma" varied within limits modeled by Lai and Katul (2000), "extkn" was allowed to vary between top-concentrated (1) and fully vertically distributed (0.01) canopy Nitrogen, and "vcmax_sc" remained within limits based on prior experimentation (V. Haverd, unpublished data). We also manually optimized parameters of a function that controls stress mortality for the tropical savannas and three of the Mediterranean woodland sites as described in Supporting Information Methods 1. We did not optimize any of the eight parameters of the Kumarathunge et al. (2019) acclimation functions or the four photosynthetic parameters of the peaked Arrhenius function because the effect of optimization parameters were found to be inseparable from the effect of other parameters. PEST converged on a parameter estimate for the four optimized parameters at all study sites (Table S3).

2.5 | Model simulations

CABLE-POP was run in offline-mode and forced with the HadGEM2-ES climate forcing from the Coupled Model Intercomparison Project 5 (CMIP5; Taylor et al., 2012). HadGEM2-ES is a configuration of the Hadley Global Environmental Model (version 2) that incorporates Earth system components (terrestrial and oceanic ecosystems, and tropospheric chemistry) with the physical atmospheric and oceanic components so that biogenic feedbacks, in particular the carbon cycle, are also modelled (Collins et al., 2011). We selected HadGEM2-ES because it scored highly at simulating Australia-wide climate in an evaluation that compared performance of CMIP5 model outputs by measuring agreement between observed and simulated climate (CSIRO and Bureau of Meteorology, 2015). Bias-corrected climate data (for bias-correction methods see Frieler et al., 2017; Lange, 2018) were downloaded from the Inter-Sectoral Impact Model Intercomparison Project (ISIMIP, simulation round Isimip2b, https://esg.pik-potsdam.de/search/isimip) for the historical period (1861–2005) and for representative concentration pathway RCP8.5 (2006–2099, "projected" period). RCP8.5 represents the most extreme climate scenario with annual global CO_2 emissions increasing to an atmospheric concentration of ~950 ppm CO_2 by 2100 (van Vuuren et al., 2011). A single climate projection was used due to lack of availability of other highly performing climate

TABLE 1 Details of the four parameters optimized at site-level using the Model-Independent Parameter Estimation Software (PEST; Doherty, 2017). Equations are duplicated from the cited references with the optimized parameter highlighted in bold text. Default value refers to the parameter value for the evergreen broadleaved forest plant functional type and was used as the starting value during optimization. Min and max value refer to the lower and upper parameter bounds provided to PEST.

Parameter	Description	Equation(s)	Default value	Min value	Max value	Reference
g1	Sensitivity of stomatal conductance (g_s) to assimilation rate (kPa$^{0.5}$) g_0 = model intercept coefficient D = vapour pressure deficit A = carbon assimilation rate C_a = atmospheric CO_2 at the leaf-surface	$g_s \approx g_0 + \left(1 + \dfrac{g_1}{\sqrt{D}}\right)\dfrac{A}{C_a}$	6	1	10	Medlyn et al. (2011)
Gamma (γ)	Sensitivity of roots and stomatal conductance to soil moisture α = root efficiency function θ = soil moisture content s = saturated w = wilting point	$\alpha(\theta) = \left(\dfrac{\theta - \theta_w}{\theta_s}\right)^{10^\gamma/(\theta - \theta_w)}$	0.00675	0.001	0.05	Lai and Katul (2000)
Extkn (k_n)	Vertical distribution of leaf nitrogen through the canopy for the two-leaf model Y = big leaf flux; L = total canopy leaf area index; y = individual leaf flux ξ = cumulative leaf area index w_i = fraction sunlit (1) or shaded (2) leaf area d = agreement index ψ = exponential function k_b = black beam radiation extinction coefficient for a black leaf canopy	$Y_i = \int_0^L y(0)\exp(-k_n\xi)w_i(\xi)d\xi = y(0)W_i$ and $W_1 = \psi\{k_b + k_n\}$ $W_2 = \psi\{k_n\} - \psi\{k_b + k_n\}$	0.4	0.1	1.0	Wang and Leuning (1998)
vcmax_sc	Scaling factor that adjusts the modelled relationship between Vc_{max} and both leaf Nitrogen (N) and leaf Phosphorus (P) (NB: the scaler is model specific and not defined by the cited reference)	$v_{cmax} = \exp(3.946 + 0.301 \times \ln(N) - 0.121 \times \ln(P) + 0.282 \times \ln(N) \times \ln(P)) \times \mathbf{vcmax\_sc}$	2.48	0.7	3.5	Walker et al. (2014)

FIGURE 2 Steps used in the parameter optimization and CABLE-POP simulations for each of the 17 wooded ecosystems. The projected period used the RCP8.5 emission scenario and simulations were repeated holding atmospheric CO_2 constant ("static CO_2").
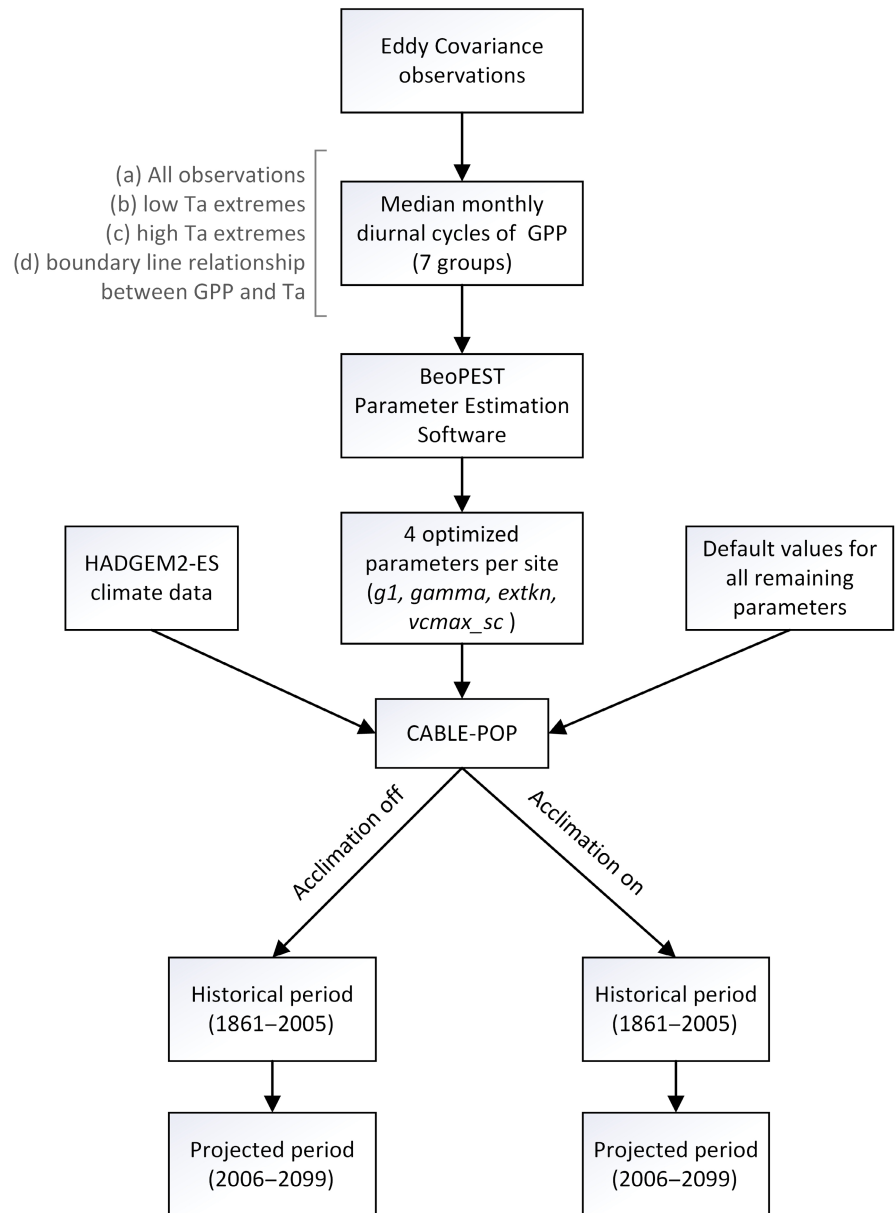
projection data. Climate data were aggregated from 0.5° to 1° and units were converted as required by the CABLE-POP input module.

We simulated average monthly carbon fluxes (GPP, NPP) and live tree carbon (aboveground and belowground) in the historical and projected periods for each of the 17 sites in separate CABLE-POP model runs—one with photosynthetic thermal acclimation and one without photosynthetic thermal acclimation. The site-specific optimized parameters were used for the simulation without photosynthetic thermal acclimation whereas parameters for E_a and ΔS of J_{max} and Vc_{max} derived from the Kumarathunge et al. (2019) functions at T_{growth} of 15°C were used for all sites for the simulation with photosynthetic thermal acclimation. We repeated simulations with "static CO_2" where CO_2 concentration was held constant at 378.8 ppm (the historical period CO_2 maximum in 2005) to explore the influence of increasing CO_2 concentration on the effect of thermal acclimation of photosynthesis. Site-specific input data included values for latitude,

longitude, canopy height, as well as forest and C_3 and C_4 grass fractions (Table 2). Grass and tree fractions (fixed throughout the simulations) were estimated following Donohue et al. (2009), who derived time series of recurrent and persistent vegetation cover (fPAR) from remote sensing data. Tree fraction was estimated as the mean maximum cover fraction across years (1982–2013) and grass fraction was set to 1- tree fraction. All other parameter values, except the stress mortality function parameters, were set to the same value per PFT for all sites. CABLE parameter, setting, and simulation output files are located at https://doi.org/10.5061/dryad.7sqv9s4wh.

2.6 | Statistical analysis

All statistical analyses were conducted in R v 3.6.2 (R Core Team, 2017). Calculation of the thermal acclimation effect

TABLE 2 Site-specific values for latitude, longitude, canopy height, and fractions of forest, grass and C4 grass used for site-level CABLE-POP simulations of historical and projected carbon fluxes. Site labels are a three letter abbreviation of the ecoregion name and the last three letters of the OzFlux site code. Ecoregion names are: MTW, Mediterranean Woodlands; SAV, Tropical savanna; TMF, Temperate Forest; TMW, Temperate Woodlands; TRF, Tropical forest. Latitude, longitude and canopy data were sourced from the OzFlux eddy covariance data files (https://dap.ozflux.org.au/thredds/catalog.html) except SAV-Dry and TMF-Wal where canopy height was sourced from Hutley et al. (2011) and https://www.ozflux.org.au, forest and grass fractions were sourced from Donohue et al. (2009), and C4 grass fractions were modelled from temperature data.

Site label	Site	Latitude (°N)	Longitude (°E)	Canopy height (m)	Forest fraction	Grass fraction	C4 grass fraction
SAV-How	Howard Springs	−12.495	131.150	16	0.502	0.498	1.0
SAV-Lit	Litchfield	−13.179	130.795	16	0.417	0.583	0.986
SAV-Ade	Adelaide River	−13.0769	131.118	16	0.378	0.622	1.0
SAV-DaS	Daly Savanna	−14.159	131.388	16	0.423	0.577	1.0
SAV-Dry	Dry River	−15.259	132.370	12	0.359	0.641	1.0
TRF-Rob	Robson Creek	−17.117	145.630	28	0.894	0.106	0.757
TRF-Ctr	Cape Tribulation	−16.103	145.447	25	0.900	0.100	0.753
MTW-Boy	Boyagin	−32.477	116.939	13	0.275	0.725	0.467
MTW-Gin	Gingin	−31.375	115.650	7	0.579	0.421	0.481
MTW-GWW	Great Western Woodlands	−30.191	120.654	18	0.293	0.707	0.729
MTW-Cpr	Calperum	−34.003	140.588	3	0.268	0.732	0.621
TMW-Cum	Cumberland Plain	−33.615	150.724	24	0.724	0.276	0.64
TMW-Whr	Whroo	−36.673	145.029	28	0.533	0.467	0.459
TMF-War	Warra	−43.095	146.655	55	0.85	0.15	0.035
TMF-Wal	Wallaby Creek	−37.426	145.188	75	0.763	0.237	0.19
TMF-Tum	Tumbarumba	−35.657	145.188	40	0.898	0.102	0.036
TMF-Wom	Wombat State Forest	−37.422	144.094	22	0.826	0.174	0.125

(Equation 5) followed the method of Sun et al. (2014). Where TAE is the thermal acclimation effect, calculated as the difference between the annual mean of C (t) in the projected period and in the historical reference period (ref, 1975–2005) between the simulation with acclimation (Acclim_on) and without acclimation (Acclim_off), and C representing daily GPP (g $Cm^{-2}day^{-1}$), daily NPP (g $Cm^{-2}day^{-1}$), or annual live tree carbon (C $Mgha^{-1}$),

$$TAE_t = (C_t - C_{ref})_{Acclim\_on} - (C_t - C_{ref})_{Acclim\_off}. \qquad (5)$$

3 | RESULTS

### 3.1 | Predicted change in MAT and MAP at the study sites

The HadGem2-ES climate model for RCP8.5 predicted site-level increases in MAT between the end of the historical (1976–2005) and end of the projected (2070–2099) period that ranged from +3.2°C (±0.07 SE, TRF-Ctr) to +4.9°C (±0.47, SAV-DaS, Figure S2a). In contrast, predicted MAP at the site level changed from an increase of +34mm (±40, SAV-DaS) to a decrease of −334mm (±66, SAV-How, Figures S2b and S3). Among ecoregions, mean changes in MAT in sites located in the two tropical ecoregions were predicted to increase by the greatest (tropical

savannas, mean: +4.6°C±0.36 95% CI) and least amounts (tropical forests, mean: +3.3°C±0.2, Figure 3a). Predicted mean MAP changes were negative in all ecoregions although 95% confidence intervals overlapped zero in the two tropical ecoregions indicating no significant change (Figure 3b).

3.2 | Site-level simulated GPP

CABLE-POP simulated an increase in mean projected GPP (2006–2099) at all sites with the exception of two Mediterranean woodlands (MTW-GWW and MTW-Cpr) where GPP for the complete timeseries (1850–2099) remained relatively flat (Figure 4). There was a clear increase in GPP in simulations with acclimation compared to those without acclimation at tropical savannas and tropical forest sites, although the effect was most pronounced at the two tropical forests (TRF-Rob and TRF-Ctr) and two of the five tropical savannas (SAV-How and SAV-Lit). In contrast, acclimation had no clear effects on the time series of simulated GPP at temperate woodlands, Mediterranean woodlands and temperate forest sites. GPP simulated by CABLE-POP closely reflected eddy-covariance observations for the majority of sites, as indicated by an overlap with mean monthly GPP observations (except TRF-Rob and TMW-Cum) and by the close agreement between the monthly means of simulated and
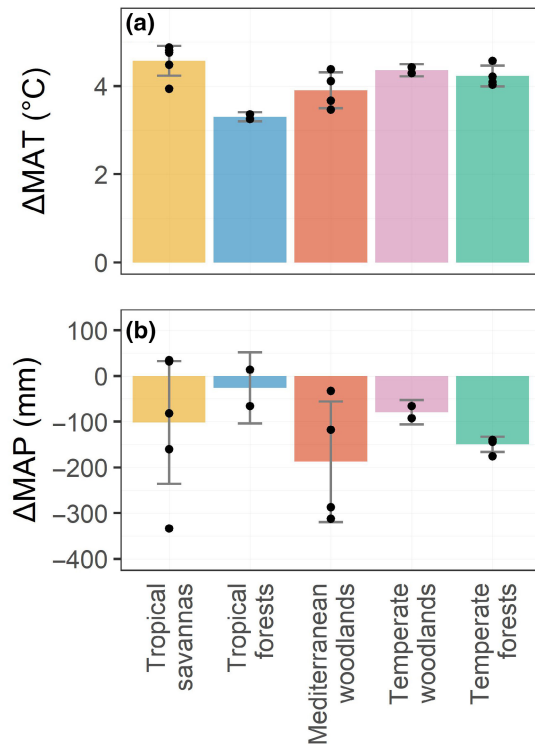
FIGURE 3 Mean change in (a) mean annual temperature (MAT) and (b) mean annual precipitation (MAP) predicted by the HadGem2-ES climate model for the RCP8.5 scenario between the end of the historical period (1976–2005) and the end of the projected period (2070–2099) for the five ecoregions represented in this study. Error bars represent 95% confidence intervals on the mean difference and black circles represent the mean difference for each of the 17 sites.

observed GPP for the observation period (i.e., $R^2 \geq 0.5$) at 14 of the 17 sites (except MTW-Gin, MTW-Cpr, and TMW-Whr, Figure S4).

3.3 | Cumulative future GPP and NPP of ecoregions

Consistent with relative divergences in simulated GPP with and without acclimation, cumulative differences in simulated GPP from 2006 to 2099 were greatest for the tropical savannas and tropical forests (Figure 5). In absolute terms, the cumulative sum of GPP in 2099 in the simulation with acclimation was higher than the simulation without acclimation by 368.9 Mg Cha^{-1} at TRF-Ctr and 316.1 Mg Cha^{-1} at TRF-Rob (Table S4). This difference between simulations was similar to the two wetter tropical savannas and substantially greater than the remaining three tropical savannas. In relative terms, the simulation with acclimation resulted in a greater increase in cumulative GPP at the tropical savannas (21.8% at SAV-Dry to 27.7% at SAV-Lit) compared to the tropical forests (8.0% at TRF-Rob and 10.7% at TRF-Ctr).

The cumulative sum of GPP revealed a small positive effect of thermal acclimation of photosynthesis that was not clearly visible in the time series at the temperate forests (51.0 to 101.8 Mg

Cha^{-1}), temperate woodlands (27.6 to 94.3 Mg Cha^{-1}) and three of the Mediterranean woodlands (3.2–19.2 Mg Cha^{-1}). In relative terms, the effect was also minor ranging from an increase in cumulative GPP of 3.2% at TMW-Cum to a decrease of −0.6% at MTW-Cpr. The effect of thermal acclimation of photosynthesis on the cumulative sum of NPP from 2006 to 2099 followed a similar pattern. The greatest absolute effect was simulated in the two wetter tropical savannas (146.7 at SAV-How and 131.3 Mg Cha^{-1} at SAV-Lit) and the two tropical forests (129.5–131.3 Mg Cha^{-1}), followed by the three drier tropical savannas (39.2–45.8 Mg ha^{-1}), temperate forests (23.7–48.8 Mg Cha^{-1}), temperate woodlands (12.7–45 Mg Cha^{-1}), and three of the Mediterranean woodlands (1.6–9.7 C Mg ha^{-1}). Similarly, the greatest relative effect was simulated at the tropical savannas (20.0% to 28.6%) followed by the tropical forests (8.2% to 10.0%) with little difference in the minor effect in the remaining ecoregions (−3.5% to 4.1%).

3.4 | Relative change in future ecoregion GPP and NPP

Consistent with absolute changes, thermal acclimation of photosynthesis led to similar patterns among ecoregions in the relative changes in mean annual GPP and NPP between the ends of the historical (1976–2005) and projected periods (2070–2099, Figure 6). There were significant differences between simulated GPP and NPP with and without acclimation for tropical savannas and tropical forests as indicated by non-overlapping 95% confidence intervals. The magnitude of this difference was greatest in tropical savannas where simulated GPP increased by 38.4% (±2.3, 95% CI) without acclimation and by 65.6% (±12.7) with acclimation (Table S5), compared with 55.3% (±3.0), without and 66.3% (±7.1) with acclimation for tropical forests. In contrast, % change in simulated GPP and NPP with and without acclimation were of similar magnitude in temperate forests, temperate woodlands, and Mediterranean woodlands indicating a minor effect of thermal acclimation of photosynthesis in these ecoregions. Similar trends were observed for the "static CO$_2$" simulation, where GPP and NPP both decreased by the end of the century for all sites except for the southern-most temperate forest (TMF-Wrr, Table S6; Figure S5). In the absence of elevated CO$_2$, thermal acclimation had the greatest effect in the tropical savannas where GPP decreased by −37.5% (±1.7) without and −22.4% (±3.1) with thermal acclimation.

3.5 | Change in seasonality of ecoregion GPP

The effect of thermal acclimation of photosynthesis on the tropical ecosystems was also clear when we examined the seasonal pattern of GPP between the end of the historical period (1976–2005) and the end of the projected period (2070–2099) for simulations with and without acclimation (Figure 7). In tropical forests, acclimation increased the seasonality of GPP by elevating GPP in the spring and
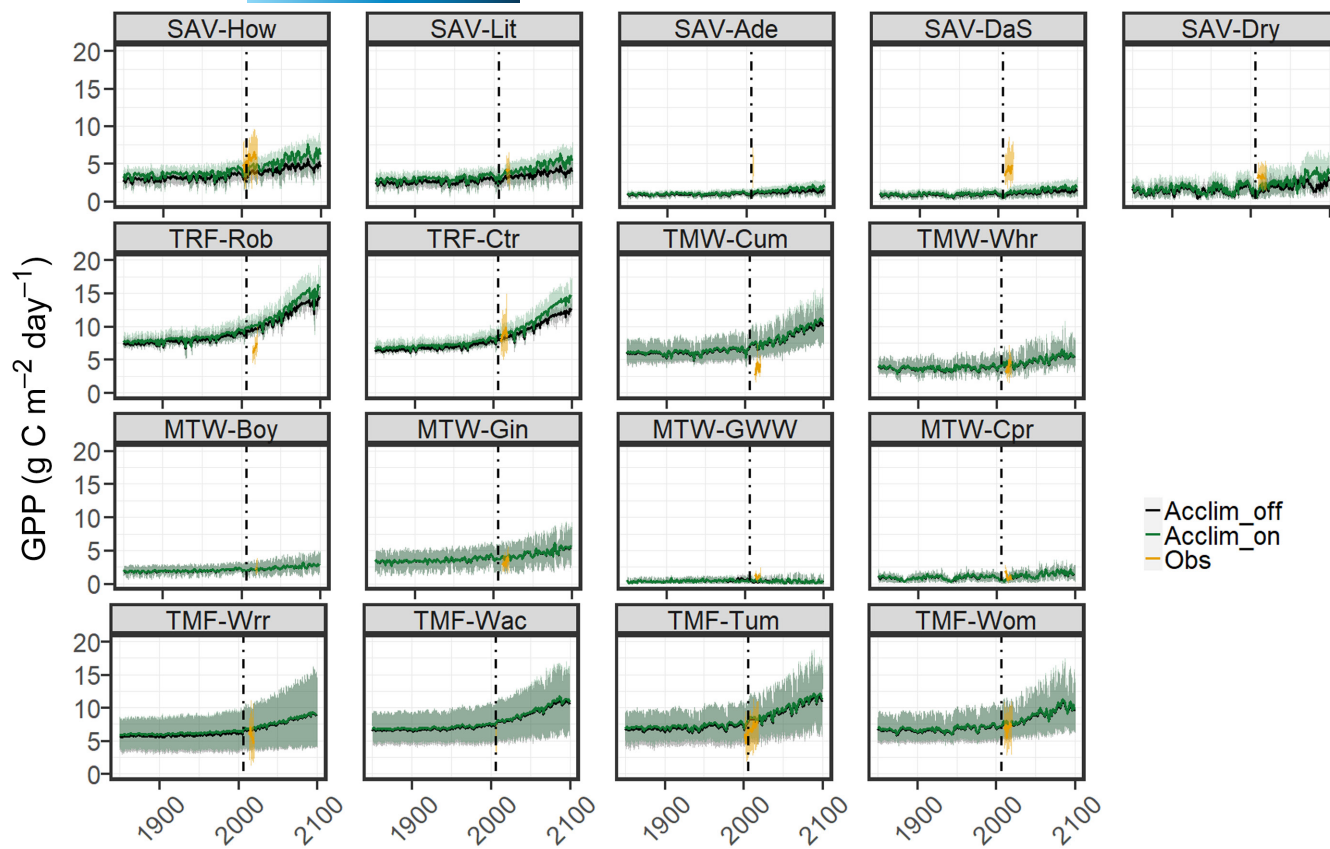
FIGURE 4 Time series of gross primary productivity (GPP; g $Cm^{-2}day^{-1}$) simulated by CABLE-POP with ("Acclim_on", green) and without ("Acclim_off", black) thermal acclimation of photosynthesis compared with eddy covariance flux observations (Obs, orange) for each of the 17 study sites. Lines represent the annual mean of daily GPP and the shaded area represents the monthly mean of daily GPP for each year. The vertical line indicates the transition between historical and projected climate data.

summer months compared to simulations without acclimation. In contrast, there were marginal increases of GPP in topical savannas that were mostly constrained to the wet season. In Mediterranean woodlands, a small increase in GPP was simulated for the cooler months in the projected period, although this did not appear to be affected by thermal acclimation and was true for only two of the four ecosystems (MTW-Boy and MTW-Gin, Figure S6). The strong seasonality of GPP in the temperate woodlands and temperate forests, where simulated GPP increased markedly in the spring and summer months was not clearly influenced by thermal acclimation of photosynthesis. In these ecoregions, GPP increased year-round in the projected period compared to the historical period for simulations with and without acclimation.

3.6 | Acclimation effect on ecoregion GPP, NPP, and biomass

The strong effect of thermal acclimation of photosynthesis on the two tropical ecoregions was further confirmed when we compared the 2006–2099 annual differences in simulated GPP, NPP, and live tree carbon storage between simulations with and without acclimation to the historical baseline (1976–2005, Figure 8; Equation 5).

In tropical forests acclimation increased GPP on average (mean TAE 2075–2099) by 1.12 (±0.28, 95% CI) μmol Cm^2s^{-1} (1.22g $Cm^{-2}day^{-1}\pm0.28$) and live tree carbon by 48.8 (±0.20) Mg Cha^{-1} (Figure 8a; Table S7). The greatest thermal acclimation effect was predicted for the end of the century in tropical forests, whereas a gradual decline after a peak in 2085 of GPP at 0.85 (±0.38) μmol Cm^2s^{-1} (0.89g $Cm^{-2}ay^{-1}\pm0.40$) and live tree carbon of 25.22 (±20.32) Mg Cha^{-1} was predicted for tropical savannas, likely due to fluctuating mortality events in one savanna ecosystem (SAV-Dry). This analysis also confirmed a small effect of thermal acclimation of photosynthesis on GPP, NPP, and live tree carbon in the temperate woodlands and a negligible effect in Mediterranean woodlands and temperate forests.

The thermal acclimation of photosynthesis effect was lower in the "static CO_2" simulations compared to the simulations where CO_2 concentrations increased under RCP8.5 (Figure 8b). On average, carbon uptake was 75% (GPP, 0.54g $Cm^{-2}day^{-1}\pm0.34$) and 78% (NPP, 0.15g $Cm^{-2}day^{-1}\pm0.07$) lower in the tropical savannas and 71% (GPP, 0.87g $Cm^{-2}day^{-1}\pm0.29$) and 74% (NPP, 0.33g $Cm^{-2}day^{-1}\pm0.04$) lower in the tropical forests over the last 30years of the projected period when the CO_2 concentration was held constant. In the remaining ecoregions GPP was between 150% (Mediterranean woodlands, 0.04g $Cm^{-2}day^{-1}\pm0.03$) and 420% (Temperate forests, 0.14g
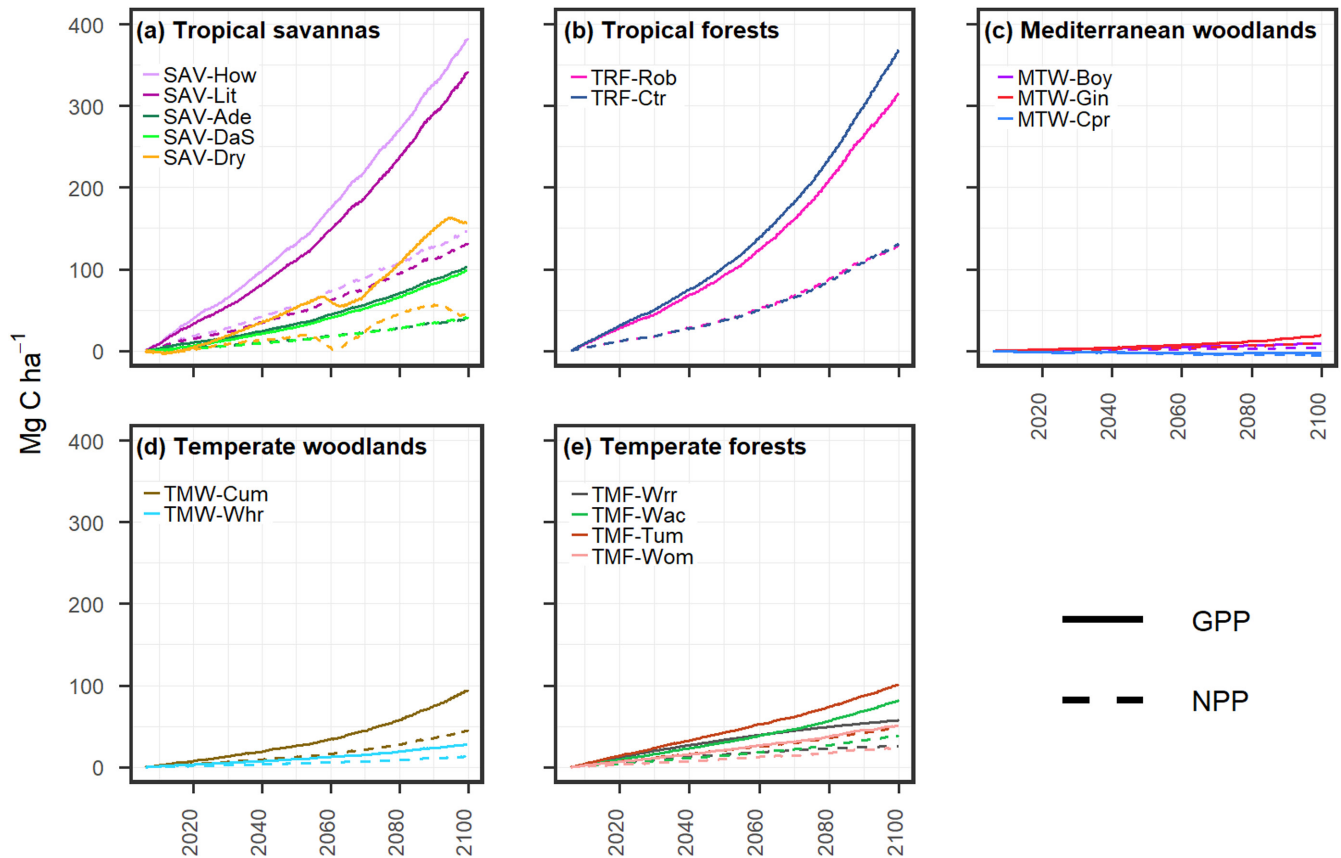
FIGURE 5 Difference in the cumulative sum of future gross primary productivity (GPP) and net primary productivity (NPP; Mg Cha^{-1}) between 2006–2099 in the simulation with and without thermal acclimation of photosynthesis for the wooded component of the 17 studied ecosystems. Positive values indicate a higher value with acclimation. Each panel represents one of the five ecoregions: (a) tropical savannas, (b) tropical forests, (c) Mediterranean woodlands, (d) temperate woodlands, and (e) temperate forests.

Cm^{-2} day^{-1} ±0.14) lower on average, although the absolute values were very small. Likewise, in all ecosystem types live tree carbon was lower at the end of the century in the "static CO_2" simulations with the decline most pronounced for the tropical forests (44.4 Mg Cha^{-1}±1.9), temperate woodlands (36.6 Mg Cha^{-1}±54.9) and tropical savannas (24.9 Mg Cha^{-1}±23.5). Overall, the "static CO_2" simulations indicated that the effect of thermal acclimation of photosynthesis on carbon uptake and storage was strongly enhanced by increasing atmospheric CO_2 concentration and that the influence of CO_2 was greatest after mid-century in the tropical savannas, tropical forests and temperate woodlands.

4 | DISCUSSION

Simulation studies that examine the effects of climate change on carbon uptake and storage in wooded ecosystems from a range of ecoregions are critical for predicting future changes to the carbon cycle. Understanding ecosystem-specific and mean ecoregion responses can facilitate planning and potentially inform policy decisions. Of key importance is understanding how climate-induced changes in ecosystem productivity can either dampen or amplify climate change. In this work, we explored the effect of a climate-induced biological response mechanism, thermal acclimation of photosynthesis, on the future GPP, NPP and live tree carbon storage in 17 Australian ecosystems from five ecoregions. By incorporating newly available thermal acclimation of photosynthesis functions (Kumarathunge et al., 2019) within the CABLE-POP LSM and modelling carbon uptake and storage to the end of the century under RCP8.5 we show that thermal acclimation of photosynthesis has a strong positive effect on GPP, NPP and live tree carbon in tropical ecoregions that is largely driven by increasing CO_2 concentrations and a negligible effect elsewhere. Furthermore, we also predict increasing GPP and NPP under climate change in all except one ecosystem. Together, these findings indicate a potential for enhanced carbon uptake under climate change that may be stronger in tropical ecoregions.

4.1 | Positive effect of climate change on GPP and NPP

Simulated GPP and NPP were enhanced under climate change (RCP8.5) by the end of the century for the majority of our study sites. Except for one Mediterranean woodland (MTW-GWW), annual carbon uptake via GPP and NPP were predicted to increase in the future, regardless of thermal acclimation of photosynthesis.
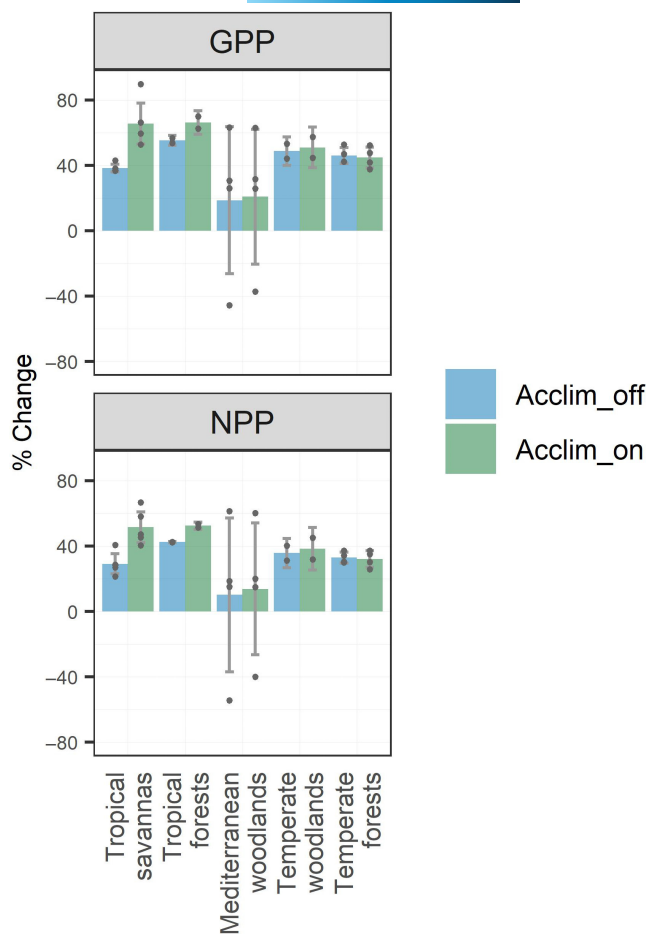
FIGURE 6 Relative change in mean annual simulated gross primary productivity (GPP) and net primary productivity (NPP; %) between the end of the historical period (1975–2005) and the end of the projected period (2070–2099) for simulations with and without thermal acclimation of photosynthesis for the five ecoregions. Error bars represent 95% confidence intervals of the mean difference and points represent the 17 sites.

Our previous work (Bennett et al., 2021) had indicated that these ecosystems may often be operating above their thermal optima of GPP under climate change potentially leading to a decline in carbon uptake rates, however simulations in this study suggest that the projected decreases in MAP (mean: −122 mm ± 27 SE) and increases in MAT (mean: +4.2°C ± 0.1, Figure 3) together with elevated atmospheric CO_2 concentration do not lead to declining carbon uptake. If our results are a true indication of future forest productivity, they suggest that (in the absence of widespread disturbances like wildfires, see below) Australian forests will continue to be a carbon sink under even the most extreme emissions scenario.

The positive effect of climate change on our predictions can be largely explained by increasing atmospheric CO_2 concentrations as confirmed by comparisons with the "static CO_2" simulations. Within our RCP8.5 simulations, CO_2 concentration increases from c. 380 ppm at the start of the projected period to c. 925 ppm in 2099, which is likely to stimulate GPP and therefore NPP via two complementary mechanisms. Firstly, there is a direct effect of CO_2 on

net carbon assimilation rates within the Farquhar et al. (1980) model of photosynthesis. At higher concentrations of atmospheric CO_2, net photosynthesis and consequently GPP is elevated when other environmental conditions remain unchanged. Secondly, Water Use Efficiency (WUE), a measure of the amount of carbon assimilated per unit of water lost to transpiration, increases with CO_2 concentration (Drake et al., 1997). Our configuration of CABLE-POP used the stomatal conductance model of Medlyn et al. (2011) within which stomatal conductance (g_s) depends directly upon atmospheric CO_2 concentration at the leaf surface (C_a, Table 1). As C_a increases there is a corresponding decrease in g_s that causes reduced transpiration losses per unit of carbon assimilated. This increase in WUE reduces the quantity of water needed for carbon assimilation as CO_2 concentrations increase, thus negating effects of decreasing water availability (i.e., reduced MAP) on simulated GPP.

The positive effect of climate change on our simulated GPP is supported by several future simulation studies at global and regional scales. For example, global carbon uptake was predicted to increase by between 11 and 320 Pg C by the end of the century under the most extreme emissions scenario in simulations with eight alternate LSM's (Arora & Boer, 2014; Friend, 2010; Sitch et al., 2008) with two (Friend, 2010; Sitch et al., 2008) attributing the changes to CO_2 fertilization (i.e., photosynthesis enhanced by elevated CO_2). At the regional scale, two Australia-wide studies that predicted effects of climate change on future carbon uptake and storage under the most extreme emission scenario both simulated NPP increases to the end of the century that were not present when CO_2 was held constant. Kelley and Harrison (2014) simulated a 56% increase in NPP compared to simulations with constant CO_2 of 380 ppm whereas Teckentrup (2023) show an approximate doubling of NPP using simulations from the CMIP6 compared to simulations with constant CO_2 of 280 ppm.

While some studies support our findings of increased productivity in woody ecosystems, uncertainties remain. Not all simulation studies report positive results and experimental studies can show lesser productivity gains than models predict. Chen and Zhuang (2013) simulated the effects of climate change on GPP and NPP across USA forests using the process-based TEM. They predicted that under the most extreme emissions scenario (A1F1) both GPP and NPP increased to mid-century and then gradually declined to the historical levels or below by the end of the century. Furthermore, the Free Air Carbon Dioxide Enrichment (FACE) experiment at TMW-Cum (EucFACE, a mature *Eucalypt* woodland) did not replicate the predicted increases in GPP simulated by the SPA model. Simulations predicted that elevated CO_2 (561 ppm) would increase GPP by between 16% and 22% (Macinnis-Ng et al., 2011) however realized GPP gains were lower (~12%, 247 g C m^{-2} year^{-1}, Jiang et al., 2020) and these did not translate into increases in aboveground NPP (ANPP, Ellsworth et al., 2017) under elevated CO_2 (ambient CO_2 + 150 ppm). This lack of increase was likely caused by nutrient limitation, which may constrain CO_2 fertilization in mature forests in the future (Norby et al., 2010; Walker et al., 2021). Given that there are already signs of a global weakening in the CO_2
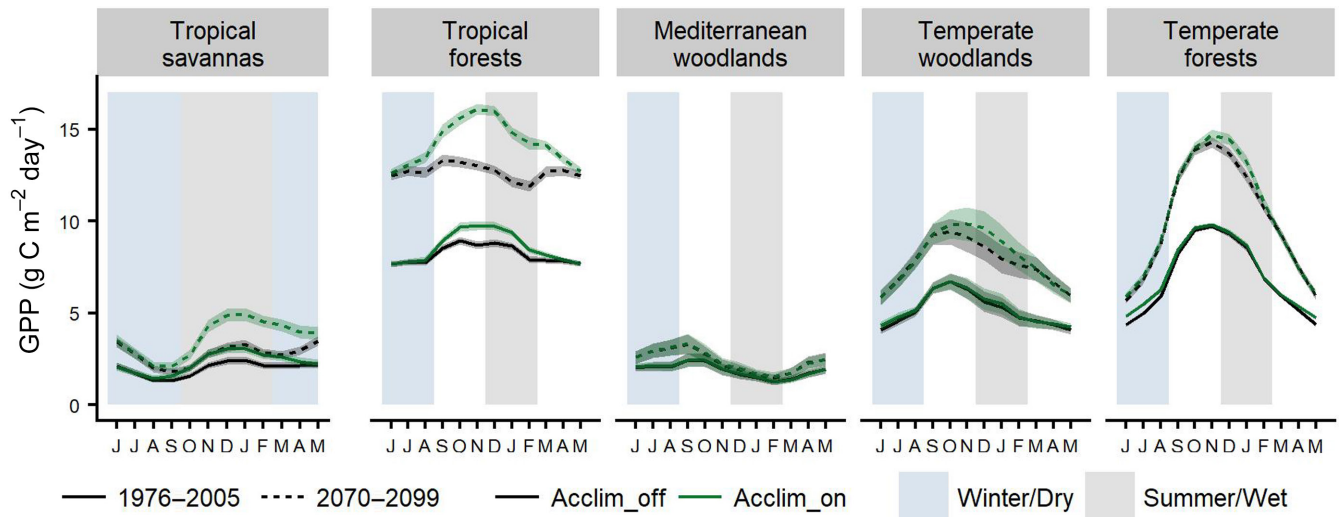
FIGURE 7 Mean monthly simulated gross primary productivity (GPP) for the end of the historical period (1976–2005, solid line) and the end of the projected period (2070–2099, dashed line) for simulations without (Acclim_off, black) and with (Acclim_on, green) acclimation for each of the five ecoregions showing changes in the seasonal pattern of GPP. Line shading represents the 95% confidence interval on the mean, and background shading indicates season.

fertilization effect (Wang, 2020) and that the effect of nutrient limitation under elevated CO_2 within CABLE-POP remains unevaluated, it is critical to interpret our results in that context.

4.2 | Strong effect of thermal acclimation of photosynthesis on tropical ecosystems

The effect of thermal acclimation of photosynthesis on simulated GPP, NPP and live tree carbon storage was strongest at the tropical sites. At the two tropical forests (TRF-Rob and TRF-Ctr) and the two wetter tropical savannas (SAV-How and SAV-Lit) the effect was sustained to the end of the century (Figure 8), with cumulative GPP and NPP of similar magnitudes (Figure 5). In both ecoregions, thermal acclimation of photosynthesis had a stronger positive influence on GPP in the warmer months, which corresponds with the wet season in tropical savannas (Figure 7). This occurred in both the historical and projected periods although climate change appeared to enhance the strength of this effect. This finding indicates that thermal acclimation of photosynthesis in tropical regions may impose negative feedbacks on the climate system. Furthermore, it implies that tropical sites are less vulnerable to temperature increases than has been suggested previously (Mau et al., 2018; Wright et al., 2009).
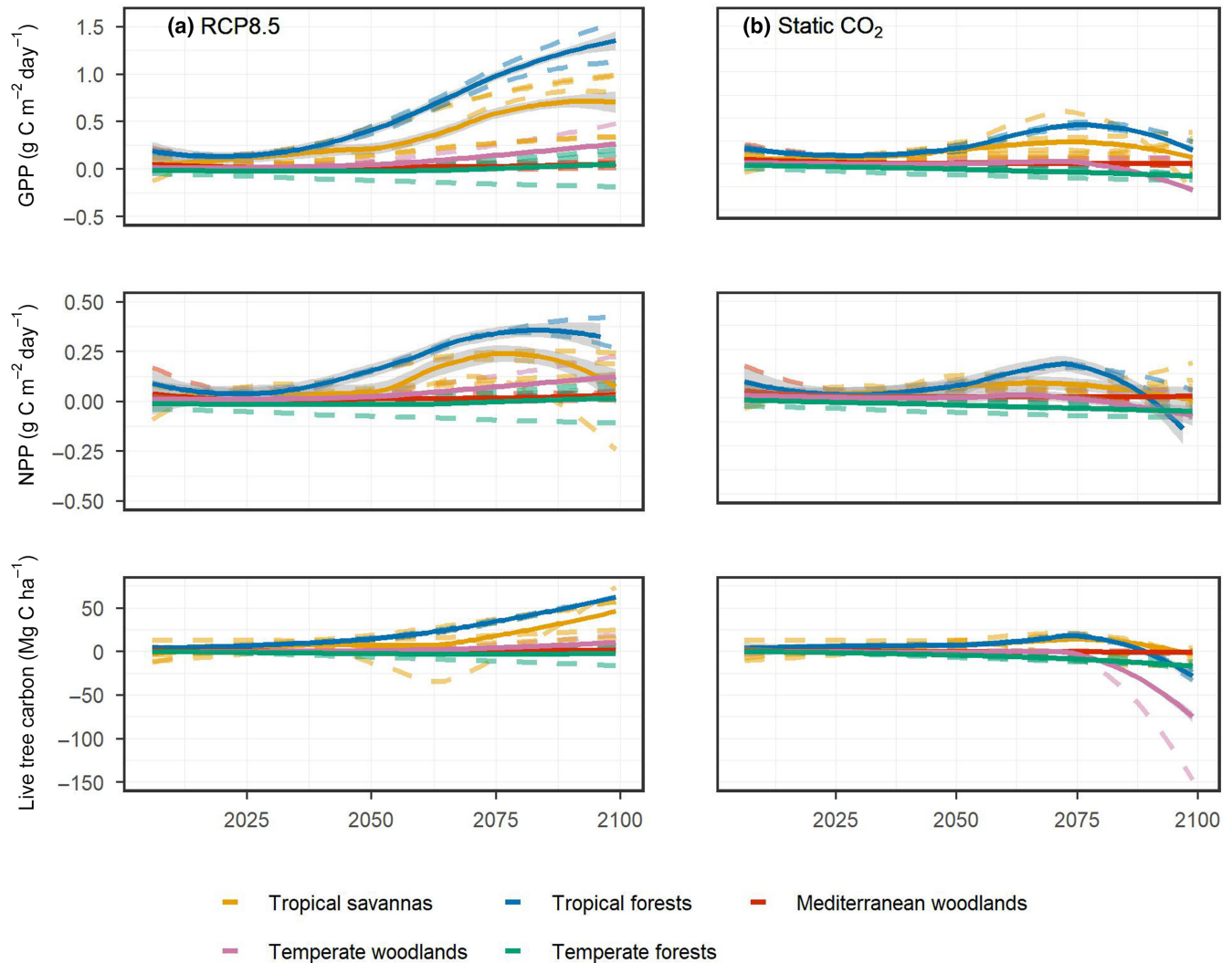
The positive effect of thermal acclimation of photosynthesis on carbon uptake and storage that was restricted to warmer regions and seasons agrees with only one of the four global simulation studies that we are aware of Mercado et al. (2018) also reported strong effects of thermal acclimation of photosynthesis on GPP and land carbon in the tropical band (Lat: 30°N to 30°S). However, the remaining three global simulation studies either partially agree with our result or contrast completely. In partial agreement, Smith et al. (2017) showed that thermal acclimation of photosynthesis imparted the

strongest effect on future average photosynthetic rates in the tropical regions (Lat: 20°N to 20°S) and in the warmer months, yet they also reported positive effects in the temperate zone (Lat: 20°N to 60°N and 20°S to 60°S). In full disagreement with our result, both Smith et al. (2016) and Lombardozzi et al. (2015) simulated negative effects of thermal acclimation of photosynthesis on vegetation carbon and land carbon gain in tropical regions with positive effects restricted to cooler regions.

These contrasting results may be attributed to alternate implementations of thermal acclimation of photosynthesis (including the method for adjusting the ratio between J_{max} and Vc_{max} [$J:V$] within the LSM). Our study is the first to use the Kumarathunge et al. (2019) functions to adjust parameters of the peaked Arrhenius equation (Equation 1) whereas previous studies used functions developed by Kattge and Knorr (2007). There are three key differences in the implementations that are likely to influence the disparity in our results. First, there is a large difference in the number of species and PFT's from which data used to develop the two functions were drawn. The Kattge and Knorr (2007) functions were developed from measurements on 36 species of broadleaved trees and shrubs, coniferous trees, and herbaceous plants of which none were from tropical forests. In contrast, the Kumarathunge et al. (2019) functions were developed from measurements on 141 species of temperate deciduous angiosperms, temperate evergreen angiosperms, temperate evergreen gymnosperms, boreal evergreen gymnosperms, tropical evergreen angiosperms, and arctic tundra of which 72 (51%) were classed as tropical evergreen angiosperms. The incorporation of tropical species is likely to have contributed to the improved predictive capacity of the Kumarathunge et al. (2019) functions in the tropical ecoregions when compared to those of Kattge and Knorr (2007).

Secondly, the method by which the ratio between J_{max} and Vc_{max} ($J:V$) was adjusted within the LSM may be influencing agreement

FIGURE 8 The thermal acclimation of photosynthesis effect (TAE) on gross primary productivity (GPP), net primary productivity (NPP), and live tree carbon storage for the projected period (2006–2099) relative to the mean historical baseline value (1976–2005) for the five ecoregions for the (a) RCP8.5 and (b) "static CO_2" simulations. The ecoregion mean (with loess smoothing applied) is represented by the solid line and individual ecosystems by the dashed lines.

with other studies. Both Kumarathunge et al. (2019) and Kattge and Knorr (2007) showed that $J{:}V$ decreases with growth temperature, yet the method for decreasing $J{:}V$ with increasing T_{growth} varies among studies. Lombardozzi et al. (2015) and Smith et al. (2016, 2017) acclimated $J{:}V$ by decreasing J_{max} at 25°C while Mercado et al. (2018) acclimated $J{:}V$ by simultaneously decreasing J_{max} and increasing Vc_{max}. In contrast, rather than acclimating $J{:}V$ to growth temperature, our implementation of "co-ordination of photosynthesis" dynamically adjusted both Vc_{max} and J_{max} to maximize photosynthesis for the previous 5 days per unit of nitrogen (Haverd et al., 2020). These three alternate methods for adjusting Vc_{max} and J_{max} to control $J{:}V$ will impact LSM photosynthetic performance at a given temperature. Adjusting $J{:}V$ by decreasing J_{max} shifts only the J_{max} temperature response function whereas adjusting $J{:}V$ by altering both J_{max} and Vc_{max} spreads the adjustment across both temperature response functions. This means that when photosynthesis is J_{max} limited, such as at higher temperatures ($\gtrsim$20°) under

elevated CO_2 concentration (Sage & Kubien, 2007), the decline in photosynthesis would be greater in the implementation where only J_{max} is adjusted leading to lower GPP, NPP and consequently carbon stores in warmer regions. This may explain the lower tropical carbon stores predicted by Lombardozzi et al. (2015) and Smith et al. (2016). Alternatively, "co-ordination of photosynthesis" influences the CO_2 fertilization effect by affecting the contribution of Vc_{max} limited photosynthesis, which is more sensitive to CO_2 concentration (Haverd et al., 2020). Thus, our implementation may have mildly enhanced the thermal acclimation effect under RCP8.5 compared to simulations where $J{:}V$ is acclimated to growth temperature as supported by Knauer et al. (2023).

Finally, the contrasting results may also be attributed to differences in the thermal range of the acclimation functions and whether LSM simulations restricted thermal acclimation of photosynthesis to within the thermal range. The range of growth temperatures in the source data used to develop the Kumarathunge et al. (2019)

functions was 3 to 37°C compared to the Kattge and Knorr (2007) functions that were 11 to 29°C for Vc_{max} and 11 to 35°C for J_{max}. Since functions were derived from measurements on plants grown within the thermal range, applying the functions to temperatures outside that range could compromise their performance (Stinziano et al., 2018). Both Smith et al. (2017) and Lombardozzi et al. (2015) restricted thermal acclimation of photosynthesis to between 11 to 35°C whereas Mercado et al. (2018) and Smith et al. (2016) did not enforce a restriction. Similarly, we placed no temperature restriction on thermal acclimation of photosynthesis, however only two of our tropical sites (SAV-Dry and SAV-Das) rarely exceeded the thermal range thus it is unlikely to have significantly compromised our results (Table S8). Though we find no obvious connection between the enforcement of a thermal restriction and agreement with our results, it is conceivable that the thermal range contributed in part to differences between the simulation studies. Overall, it is likely that the combined effects of alternate implementations of thermal acclimation of photosynthesis, together with different LSM's and climate forcings contribute to the regional variation in thermal acclimation of photosynthesis effect between studies.

4.3 | Study limitations

It is important to interpret our results in light of limitations in our model implementation, CABLE-POP, and current ecological knowledge. First, though we simulated regular disturbances in CABLE-POP, disturbances were not explicitly linked to predicted changes in fire regimes or pest and disease outbreaks which are likely to increase in frequency and severity in Australian forests under climate change and cause negative effects on forest carbon uptake and storage (Booth et al., 2015; Bowman et al., 2020; Pinkard et al., 2017). Changed fire regimes are of particular importance since recent changes in fire weather (~ last 30 years) have been linked to large (~350%) increases in forest area burned across Australia with these trends expected to continue under climate change (Canadell et al., 2021). Secondly, CABLE parameters for the Evergreen Broadleaf Forest PFT were optimized against eddy-covariance observations of GPP and ET that were derived from whole ecosystems that included both tree and grass components. This may have biased the optimization, particularly for the tropical savanna ecosystems where the grass fraction ranged from ~0.5 to 0.6 (Table 2) and C4 grasses contribute around half of GPP during the wet season (Ma et al., 2020; Moore et al., 2016). Finally, our implementation of the thermal acclimation of photosynthesis functions will have influenced the simulated thermal acclimation effect. Acclimation outside the function's thermal range may have enhanced the effect at very high and low temperatures; adjusting J:V through "co-ordination of photosynthesis" eliminated thermal acclimation effects on this ratio; and including both the effects of acclimation and adaptation from the Kumarathunge et al. (2019) functions incorporated effects of adaptation within the reported thermal acclimation effect which may be of particular importance when photosynthesis was limited by J_{max}.

Like all LSM's CABLE-POP is also limited in its ability to simulate several components of ecosystem carbon dynamics. For example, photosynthesis has been widely observed to acclimate to elevated CO_2 in experimental conditions (Ainsworth & Long, 2005; Ainsworth & Rogers, 2007). In CABLE-POP, CO_2 concentration is a key input to the photosynthesis functions, however these functions do not acclimate with changing CO_2 concentration. Likewise, the CABLE-POP biomass allocation scheme may not accurately represent the conversion of GPP into live tree biomass under elevated CO_2. True carbon assimilation is limited either by CO_2 availability (i.e., source limited) or cambial cell growth (i.e., sink limited, Cabon et al., 2022) and while elevated CO_2 likely stimulated GPP via the Farquhar et al. (1980) photosynthesis model, whether the stem biomass allocation scheme of Shinozaki et al. (1964)'s pipe model accurately represents conversion of GPP to biomass under conditions of elevated CO_2 is unknown. Furthermore, CABLE-POP acclimates leaf, stem and root respiration to changing temperature but not to changing CO_2 concentration despite experimental evidence that plant respiration can be influenced by CO_2 concentration (Dusenge et al., 2019). As such, real-world responses to elevated CO_2 may deviate from our predictions.

Additional uncertainties in our study relate to insufficient knowledge of ecosystem responses to the novel environmental conditions of climate change. As noted above, the capacity for plants to acclimate photosynthesis beyond the 37°C upper limit of the Kumarathunge et al. (2019) functions is currently unknown. This will be key to understanding whether tropical ecosystems are able to acclimate in situ as the climate warms. Likewise, there are a lack of data on photosynthetic thermal acclimation of C_4 grasses which is of particular importance for tropical savanna ecosystems. Yamori et al. (2014) demonstrated that the photosynthetic thermal optima of C_4 plants is linearly related to growth temperature which implies thermal acclimation. However, functions for simulating C_4 acclimation within LSM's have not yet been developed. Finally, of critical importance to improving the representation of future carbon uptake and storage under climate change within LSMs is advancing our knowledge of the interactive effects of acclimation to both elevated CO_2 and temperature on photosynthetic parameters.

5 | CONCLUSION

Our study is the first to simulate the effects of thermal acclimation of photosynthesis on future GPP, NPP, and live tree carbon storage in diverse wooded ecosystems under climate change using functions developed by Kumarathunge et al. (2019). We show that thermal acclimation of photosynthesis would enhance carbon uptake and storage in tropical savannas and tropical forests and have small or negligible effects in Mediterranean woodlands, temperate woodlands, and temperate forests. Our simulations indicate that this enhancement is largely stimulated by projected increases in atmospheric CO_2 concentrations. Furthermore, our simulations suggest that the combined direct effects of increasing

temperatures, changed precipitation regimes, and elevated CO_2 will enhance GPP, NPP and live tree carbon storage across a range of wooded ecosystems in the future. While our results give reason to be cautiously optimistic, improved representation of the effects of nutrient limitation, photosynthetic acclimation to elevated CO_2, and intensified disturbance regimes will be critical to improving future simulations of carbon uptake and storage in Australia's wooded ecosystems.

AUTHOR CONTRIBUTIONS

ACKNOWLEDGEMENTS

CONFLICT OF INTEREST STATEMENT

The authors declare no conflicts of interest.

DATA AVAILABILITY STATEMENT

The data that support the findings of this study are openly available in Dryad at https://doi.org/10.5061/dryad.7sqv9s4wh.

ORCID

Alison C. Bennett https://orcid.org/0000-0002-8249-976X
Jürgen Knauer https://orcid.org/0000-0002-4947-7067
Lauren T. Bennett https://orcid.org/0000-0003-2472-062X
Vanessa Haverd https://orcid.org/0000-0003-4359-5895
Stefan K. Arndt https://orcid.org/0000-0001-7086-9375

REFERENCES

Ainsworth, E. A., & Long, S. P. (2005). What have we learned from 15 years of free-air CO_2 enrichment (FACE)? A meta-analytic review of the responses of photosynthesis, canopy properties and plant production to rising CO_2. *New Phytologist*, *165*(2), 351–371. https://doi.org/10.1111/j.1469-8137.2004.01224.x

Ainsworth, E. A., & Rogers, A. (2007). The response of photosynthesis and stomatal conductance to rising CO_2: Mechanisms and environmental interactions. *Plant Cell and Environment*, *30*(3), 258–270. https://doi.org/10.1111/j.1365-3040.2007.01641.x

Arias, P. A., Bellouin, N., Coppola, E., Jones, R. G., Krinner, G., Marotzke, J., Naik, V., Palmer, M. D., Plattner, G.-K., Rogelj, J., Rojas, M., Sillmann, J., Storelvmo, T., Thorne, P. W., Trewin, B., Rao, K. A., Adhikary, B., Allan, R. P., Armour, K., ... Zickfeld, K. (2021). Technical summary. In V. Masson-Delmotte, P. Zhai, A. Pirani, S. L. Connors, C. Péan, S. Berger, N. Caud, Y. Chen, M. I. G. L. Goldfarb, M. Huang, K. Leitzell, E. Lonnoy, J. B. R. Matthews, T. K. Maycock, T. Waterfield, O. Yelekçi, R. Yu, & A. B. Zhou (Eds.), *Climate change 2021: The physical science basis. Contribution of working group I to the sixth assessment report of the intergovernmental panel on climate change* (pp. 33–144). Cambridge University Press. https://doi.org/10.1017/9781009157896.002

Arneth, A., Mercado, L., Kattge, J., & Booth, B. B. B. (2012). Future challenges of representing land-processes in studies on land-atmosphere interactions. *Biogeosciences*, *9*(9), 3587–3599. https://doi.org/10.5194/bg-9-3587-2012

Arora, V. K., & Boer, G. J. (2014). Terrestrial ecosystems response to future changes in climate and atmospheric CO_2 concentration. *Biogeosciences*, *11*(15), 4157–4171. https://doi.org/10.5194/bg-11-4157-2014

Aspinwall, M. J., Drake, J. E., Campany, C., Varhammar, A., Ghannoum, O., Tissue, D. T., Reich, P. B., & Tjoelker, M. G. (2016). Convergent acclimation of leaf photosynthesis and respiration to prevailing ambient temperatures under current and warmer climates in *Eucalyptus tereticornis*. *New Phytologist*, *212*(2), 354–367. https://doi.org/10.1111/nph.14035

Atkin, O. K., Bloomfield, K. J., Reich, P. B., Tjoelker, M. G., Asner, G. P., Bonal, D., Bonisch, G., Bradford, M. G., Cernusak, L. A., Cosio, E. G., Creek, D., Crous, K. Y., Domingues, T. F., Dukes, J. S., Egerton, J. J. G., Evans, J. R., Farquhar, G. D., Fyllas, N. M., Gauthier, P. P. G., ... Zaragoza-Castells, J. (2015). Global variability in leaf respiration in relation to climate, plant functional types and leaf traits. *New Phytologist*, *206*(2), 614–636. https://doi.org/10.1111/nph.13253

Bennett, A. C., Arndt, S. K., Bennett, L. T., Knauer, J., Beringer, J., Griebel, A., Hinko-Najera, N., Liddell, M. J., Metzen, D., Pendall, E., Silberstein, R. P., Wardlaw, T. J., Woodgate, W., & Haverd, V. (2021). Thermal optima of gross primary productivity are closely aligned with mean air temperatures across Australian wooded ecosystems. *Global Change Biology*, *27*(19), 4727–4744. https://doi.org/10.1111/gcb.15760

Bennett, A. C., Penman, T. D., Arndt, S. K., Roxburgh, S. H., & Bennett, L. T. (2020). Climate more important than soils for predicting forest biomass at the continental scale. *Ecography*, *43*(11), 1692–1705. https://doi.org/10.1111/ecog.05180

Beringer, J., Hutley, L. B., McHugh, I., Arndt, S. K., Campbell, D., Cleugh, H. A., Cleverly, J., de Dios, V. R., Eamus, D., Evans, B., Ewenz, C., Grace, P., Griebel, A., Haverd, V., Hinko-Najera, N., Huete, A., Isaac, P., Kanniah, K., Leuning, R., ... Wardlaw, T. (2016). An introduction to the Australian and New Zealand flux tower network—OzFlux. *Biogeosciences*, *13*(21), 5895–5916. https://doi.org/10.5194/bg-13-5895-2016

Beringer, J., Moore, C. E., Cleverly, J., Campbell, D. I., Cleugh, H., De Kauwe, M. G., Kirschbaum, M. U. F., Griebel, A., Grover, S., Huete, A., Hutley, L. B., Laubach, J., Van Niel, T., Arndt, S. K., Bennett, A. C., Cernusak, L. A., Eamus, D., Ewenz, C. M., Goodrich, J. P., ... Woodgate, W. (2022). Bridge to the future: Important lessons from 20 years of ecosystem observations made by the OzFlux network. *Global Change Biology*, *28*(11), 3489–3514. https://doi.org/10.1111/gcb.16141

Bermudez, R., Stefanski, A., Montgomery, R. A., & Reich, P. B. (2021). Short- and long-term responses of photosynthetic capacity to temperature in four boreal tree species in a free-air warming and rainfall manipulation experiment. *Tree Physiology*, 41(1), 89–102. https://doi.org/10.1093/treephys/tpaa115

Booth, B. B. B., Jones, C. D., Collins, M., Totterdell, I. J., Cox, P. M., Sitch, S., Huntingford, C., Betts, R. A., Harris, G. R., & Lloyd, J. (2012). High sensitivity of future global warming to land carbon cycle processes. *Environmental Research Letters*, 7(2), 1–8. https://doi.org/10.1088/1748-9326/7/2/024002

Booth, T. H., Broadhurst, L. M., Pinkard, E., Prober, S. M., Dillon, S. K., Bush, D., Pinyopusarerk, K., Doran, J. C., Ivkovich, M., & Young, A. G. (2015). Native forests and climate change: Lessons from eucalypts. *Forest Ecology and Management*, 347, 18–29. https://doi.org/10.1016/j.foreco.2015.03.002

Bowman, D., Kolden, C. A., Abatzoglou, J. T., Johnston, F. H., van der Werf, G. R., & Flannigan, M. (2020). Vegetation fires in the Anthropocene. *Nature Reviews Earth & Environment*, 1(10), 500–515. https://doi.org/10.1038/s43017-020-0085-3

Bureau of Meteorology. (2020). *Climate classification of Australia*. Australian Government Bureau of Meteorology. http://www.bom.gov.au/jsp/ncc/climate_averages/climate-classifications/index.jsp?maptype=kpngrp#maps

Cabon, A., Kannenberg, S. A., Arain, A., Babst, F., Baldocchi, D., Belmecheri, S., Delpierre, N., Guerrieri, R., Maxwell, J. T., McKenzie, S., Meinzer, F. C., Moore, D. J. P., Pappas, C., Rocha, A. V., Szejner, P., Ueyama, M., Ulrich, D., Vincke, C., Voelker, S. L., ... Anderegg, W. R. L. (2022). Cross-biome synthesis of source versus sink limits to tree growth. *Science*, 376(6594), 758–761. https://doi.org/10.1126/science.abm4875

Cai, W. W., Yuan, W. P., Liang, S. L., Liu, S. G., Dong, W. J., Chen, Y., Liu, D., & Zhang, H. C. (2014). Large differences in terrestrial vegetation production derived from satellite-based light use efficiency models. *Remote Sensing*, 6(9), 8945–8965. https://doi.org/10.3390/rs6098945

Canadell, J. G., Meyer, C. P., Cook, G. D., Dowdy, A., Briggs, P. R., Knauer, J., Pepler, A., & Haverd, V. (2021). Multi-decadal increase of forest burned area in Australia is linked to climate change. *Nature Communications*, 12(1), 6921. https://doi.org/10.1038/s41467-021-27225-4

Chen, J. L., Reynolds, J. F., Harley, P. C., & Tenhunen, J. D. (1993). Coordination theory of leaf nitrogen distribution in a canopy. *Oecologia*, 93(1), 63–69. https://doi.org/10.1007/bf00321192

Chen, M., & Zhuang, Q. L. (2013). Modelling temperature acclimation effects on the carbon dynamics of forest ecosystems in the conterminous United States. *Tellus Series B-Chemical and Physical Meteorology*, 65, 19156. https://doi.org/10.3402/tellusb.v65i0.19156

Collins, W. J., Bellouin, N., Doutriaux-Boucher, M., Gedney, N., Halloran, P., Hinton, T., Hughes, J., Jones, C. D., Joshi, M., Liddicoat, S., Martin, G., O'Connor, F., Rae, J., Senior, C., Sitch, S., Totterdell, I., Wiltshire, A., & Woodward, S. (2011). Development and evaluation of an earth-system model-HadGEM2. *Geoscientific Model Development*, 4(4), 1051–1075. https://doi.org/10.5194/gmd-4-1051-2011

CSIRO and Bureau of Meteorology. (2015). *Climate change in Australia: Information for Australia's natural resource management regions: Technical report*. CSIRO and Bureau of Meteorology.

De Kauwe, M. G., Medlyn, B. E., Zaehle, S., Walker, A. P., Dietze, M. C., Wang, Y. P., Luo, Y. Q., Jain, A. K., El-Masri, B., Hickler, T., Warlind, D., Weng, E. S., Parton, W. J., Thornton, P. E., Wang, S. S., Prentice, I. C., Asao, S., Smith, B., McCarthy, H. R., ... Norby, R. J. (2014). Where does the carbon go? A model-data intercomparison of vegetation carbon allocation and turnover processes at two temperate forest free-air CO_2 enrichment sites. *New Phytologist*, 203(3), 883–899. https://doi.org/10.1111/nph.12847

Department of Agriculture Water and the Environment. (2018). *Interim Biogeographic Regionalisation for Australia v. 7 (IBRA) [ESRI shapefile]*. Commonwealth of Australia. http://www.environment.gov.au/fed/catalog/search/resource/details.page?uuid=%7B4A2321F0-DD57-454E-BE34-6FD4BDE64703%7D

Dillaway, D. N., & Kruger, E. L. (2010). Thermal acclimation of photosynthesis: A comparison of boreal and temperate tree species along a latitudinal transect. *Plant Cell and Environment*, 33(6), 888–899. https://doi.org/10.1111/j.1365-3040.2010.02114.x

Doherty, J. (2017). *PEST: Model-independent parameter estimation and uncertainty analysis*. Watermark Computing.

Donohue, R. J., McVicar, T. R., & Roderick, M. L. (2009). Climate-related trends in Australian vegetation cover as inferred from satellite observations, 1981–2006. *Global Change Biology*, 15(4), 1025–1039. https://doi.org/10.1111/j.1365-2486.2008.01746.x

Drake, B. G., GonzalezMeler, M. A., & Long, S. P. (1997). More efficient plants: A consequence of rising atmospheric CO_2? *Annual Review of Plant Physiology and Plant Molecular Biology*, 48, 609–639. https://doi.org/10.1146/annurev.arplant.48.1.609

Drake, J. E., Aspinwall, M. J., Pfautsch, S., Rymer, P. D., Reich, P. B., Smith, R. A., Crous, K. Y., Tissue, D. T., Ghannoum, O., & Tjoelker, M. G. (2015). The capacity to cope with climate warming declines from temperate to tropical latitudes in two widely distributed *Eucalyptus* species. *Global Change Biology*, 21(1), 459–472. https://doi.org/10.1111/gcb.12729

Drake, J. E., Tjoelker, M. G., Aspinwall, M. J., Reich, P. B., Barton, C. V. M., Medlyn, B. E., & Duursma, R. A. (2016). Does physiological acclimation to climate warming stabilize the ratio of canopy respiration to photosynthesis? *New Phytologist*, 211(3), 850–863. https://doi.org/10.1111/nph.13978

Dusenge, M. E., Duarte, A. G., & Way, D. A. (2019). Plant carbon metabolism and climate change: Elevated CO_2 and temperature impacts on photosynthesis, photorespiration and respiration. *New Phytologist*, 221(1), 32–49. https://doi.org/10.1111/nph.15283

Ellsworth, D. S., Anderson, I. C., Crous, K. Y., Cooke, J., Drake, J. E., Gherlenda, A. N., Gimeno, T. E., Macdonald, C. A., Medlyn, B. E., Powell, J. R., Tjoelker, M. G., & Reich, P. B. (2017). Elevated CO_2 does not increase *eucalypt* forest productivity on a low-phosphorus soil. *Nature Climate Change*, 7(4), 279–283. https://doi.org/10.1038/nclimate3235

Farquhar, G. D., Caemmerer, S. V., & Berry, J. A. (1980). A biochemical-model of photosynthetic CO_2 assimilation in leaves of C-3 species. *Planta*, 149(1), 78–90. https://doi.org/10.1007/bf00386231

Friedlingstein, P., O'Sullivan, M., Jones, M. W., Andrew, R. M., Gregor, L., Hauck, J., Le Quere, C., Luijkx, I. T., Olsen, A., Peters, G. P., Peters, W., Pongratz, J., Schwingshackl, C., Sitch, S., Canadell, J. G., Ciais, P., Jackson, R. B., Alin, S. R., Alkama, R., ... Zheng, B. (2022). Global carbon budget 2022. *Earth System Science Data*, 14(11), 4811–4900. https://doi.org/10.5194/essd-14-4811-2022

Frieler, K., Lange, S., Piontek, F., Reyer, C. P. O., Schewe, J., Warszawski, L., Zhao, F., Chini, L., Denvil, S., Emanuel, K., Geiger, T., Halladay, K., Hurtt, G., Mengel, M., Murakami, D., Ostberg, S., Popp, A., Riva, R., Stevanovic, M., ... Yamagata, Y. (2017). Assessing the impacts of 1.5 degrees C global warming—Simulation protocol of the Inter-Sectoral Impact Model Intercomparison Project (ISIMIP2b). *Geoscientific Model Development*, 10(12), 4321–4345. https://doi.org/10.5194/gmd-10-4321-2017

Friend, A. D. (2010). Terrestrial plant production and climate change. *Journal of Experimental Botany*, 61(5), 1293–1309. https://doi.org/10.1093/jxb/erq019

Groenendijk, M., Dolman, A. J., van der Molen, M. K., Leuning, R., Arneth, A., Delpierre, N., Gash, J. H. C., Lindroth, A., Richardson, A. D., Verbeeck, H., & Wohlfahrt, G. (2011). Assessing parameter variability in a photosynthesis model within and between plant functional types using global Fluxnet eddy covariance data. *Agricultural and*

Forest Meteorology, *151*(1), 22–38. https://doi.org/10.1016/j.agrformet.2010.08.013

Gunderson, C. A., O'Hara, K. H., Campion, C. M., Walker, A. V., & Edwards, N. T. (2010). Thermal plasticity of photosynthesis: The role of acclimation in forest responses to a warming climate. *Global Change Biology*, *16*(8), 2272–2286. https://doi.org/10.1111/j.1365-2486.2009.02090.x

Haverd, V., Raupach, M. R., Briggs, P. R., Canadell, J. G., Isaac, P., Pickett-Heaps, C., Roxburgh, S. H., van Gorsel, E., Rossel, R. A. V., & Wang, Z. (2013). Multiple observation types reduce uncertainty in Australia's terrestrial carbon and water cycles. *Biogeosciences*, *10*(3), 2011–2040. https://doi.org/10.5194/bg-10-2011-2013

Haverd, V., Smith, B., Canadell, J. G., Cuntz, M., Mikaloff-Fletcher, S., Farquhar, G., Woodgate, W., Briggs, P. R., & Trudinger, C. M. (2020). Higher than expected CO_2 fertilization inferred from leaf to global observations. *Global Change Biology*, *26*(4), 2390–2402. https://doi.org/10.1111/gcb.14950

Haverd, V., Smith, B., Cook, G. D., Briggs, P. R., Nieradzik, L., Roxburgh, S. H., Liedloff, A., Meyer, C. P., & Canadell, J. G. (2013). A stand-alone tree demography and landscape structure module for Earth system models. *Geophysical Research Letters*, *40*(19), 5234–5239. https://doi.org/10.1002/grl.50972

Haverd, V., Smith, B., Nieradzik, L., Briggs, P. R., Woodgate, W., Trudinger, C. M., Canadell, J. G., & Cuntz, M. (2018). A new version of the CABLE land surface model (subversion revision r4601), incorporating land use and land cover change, woody vegetation demography, and a novel optimisation-based approach to plant coordination of photosynthesis. *Geoscientific Model Development*, *11*, 2995–3026. https://doi.org/10.5194/gmd-11-2995-2018

Haverd, V., Smith, B., Nieradzik, L. P., & Briggs, P. R. (2014). A stand-alone tree demography and landscape structure module for Earth system models: Integration with inventory data from temperate and boreal forests. *Biogeosciences*, *11*(15), 4039–4055. https://doi.org/10.5194/bg-11-4039-2014

Huang, M. T., Piao, S. L., Ciais, P., Penuelas, J., Wang, X. H., Keenan, T. F., Peng, S. S., Berry, J. A., Wang, K., Mao, J. F., Alkama, R., Cescatti, A., Cuntz, M., De Deurwaerder, H., Gao, M. D., He, Y., Liu, Y. W., Luo, Y. Q., Myneni, R. B., … Janssens, I. A. (2019). Air temperature optima of vegetation productivity across global biomes. *Nature Ecology & Evolution*, *3*(5), 772–779. https://doi.org/10.1038/s41559-019-0838-x

Hutley, L. B., Beringer, J., Isaac, P. R., Hacker, J. M., & Cernusak, L. A. (2011). A sub-continental scale living laboratory: Spatial patterns of savanna vegetation over a rainfall gradient in northern Australia. *Agricultural and Forest Meteorology*, *151*(2011), 1417–1428.

IPCC. (2021). Summary for policymakers. In V. Masson-Delmotte, P. Zhai, A. Pirani, S. L. Connors, C. Péan, S. Berger, N. Caud, Y. Chen, L. Goldfarb, M. I. Gomis, M. Huang, K. Leitzell, E. Lonnoy, J. B. R. Matthews, T. K. Maycock, T. Waterfield, O. Yelekçi, R. Yu, & B. Zhou (Eds.), *Climate change 2021: The physical science basis. Contribution of working group I to the sixth assessment report of the Intergovernmental Panel on Climate Change* (pp. 3–32). Cambridge University Press. https://doi.org/10.1017/9781009157896.001

Jiang, M. K., Medlyn, B. E., Drake, J. E., Duursma, R. A., Anderson, I. C., Barton, C. V. M., Boer, M. M., Carrillo, Y., Castaneda-Gomez, L., Collins, L., Crous, K. Y., De Kauwe, M. G., dos Santos, B. M., Emmerson, K. M., Facey, S. L., Gherlenda, A. N., Gimeno, T. E., Hasegawa, S., Johnson, S. N., … Ellsworth, D. S. (2020). The fate of carbon in a mature forest under carbon dioxide enrichment. *Nature*, *580*(7802), 227. https://doi.org/10.1038/s41586-020-2128-9

Johnson, F. H., Eyring, H., & Williams, R. W. (1942). The nature of enzyme inhibitions in bacterial luminescence—Sulfanilamide, urethane, temperature and pressure. *Journal of Cellular and Comparative Physiology*, *20*(3), 247–268. https://doi.org/10.1002/jcp.1030200302

Kattge, J., & Knorr, W. (2007). Temperature acclimation in a biochemical model of photosynthesis: A reanalysis of data from 36 species. *Plant Cell and Environment*, *30*(9), 1176–1190. https://doi.org/10.1111/j.1365-3040.2007.01690.x

Kelley, D. I., & Harrison, S. P. (2014). Enhanced Australian carbon sink despite increased wildfire during the 21st century. *Environmental Research Letters*, *9*(10), 1–10. https://doi.org/10.1088/1748-9326/9/10/104015

Knauer, J., Smith, B., Medlyn, B., Canadell, J., Haverd, V., Cuntz, M., Bennett, A. C., & Caldararu, S. (2023). *Higher response of gross primary productivity under future climate with more comprehensive representations of photosynthesis*. Science Advances. https://doi.org/10.1126/sciadv.adh9444

Kohl, M., Lasco, R., Cifuentes, M., Jonsson, O., Korhonen, K. T., Mundhenk, P., Navar, J. D., & Stinson, G. (2015). Changes in forest production, biomass and carbon: Results from the 2015 UN FAO global Forest resource assessment. *Forest Ecology and Management*, *352*, 21–34. https://doi.org/10.1016/j.foreco.2015.05.036

Kolari, P., Chan, T., Porcar-Castell, A., Back, J., Nikinmaa, E., & Juurola, E. (2014). Field and controlled environment measurements show strong seasonal acclimation in photosynthesis and respiration potential in boreal scots pine. *Frontiers in Plant Science*, *5*, 717. https://doi.org/10.3389/fpls.2014.00717

Kumarathunge, D. P., Medlyn, B. E., Drake, J. E., Tjoelker, M. G., Aspinwall, M. J., Battaglia, M., Cano, F. J., Carter, K. R., Cavaleri, M. A., Cernusak, L. A., Chambers, J. Q., Crous, K. Y., De Kauwe, M. G., Dillaway, D. N., Dreyer, E., Ellsworth, D. S., Ghannoum, O., Han, Q. M., Hikosaka, K., … Way, D. A. (2019). Acclimation and adaptation components of the temperature dependence of plant photosynthesis at the global scale. *New Phytologist*, *222*(2), 768–784. https://doi.org/10.1111/nph.15668

Lai, C. T., & Katul, G. (2000). The dynamic role of root-water uptake in coupling potential to actual transpiration. *Advances in Water Resources*, *23*(4), 427–439. https://doi.org/10.1016/s0309-1708(99)00023-8

Lange, S. (2018). Bias correction of surface downwelling longwave and shortwave radiation for the EWEMBI dataset. *Earth System Dynamics*, *9*(2), 627–645. https://doi.org/10.5194/esd-9-627-2018

Li, Y. Y., Liu, J. X., Zhou, G. Y., Huang, W. J., & Duan, H. L. (2016). Warming effects on photosynthesis of subtropical tree species: A translocation experiment along an altitudinal gradient. *Scientific Reports*, *6*, 24895. https://doi.org/10.1038/srep24895

Lin, Y.-S., Medlyn, B. E., De Kauwe, M. G., & Ellsworth, D. S. (2013). Biochemical photosynthetic responses to temperature: How do interspecific differences compare with seasonal shifts? *Tree Physiology*, *33*(8), 793–806. https://doi.org/10.1093/treephys/tpt047

Lin, Y. S., Medlyn, B. E., Duursma, R. A., Prentice, I. C., Wang, H., Baig, S., Eamus, D., de Dios, V. R., Mitchell, P., Ellsworth, D. S., Op de Beeck, M., Wallin, G., Uddling, J., Tarvainen, L., Linderson, M. L., Cernusak, L. A., Nippert, J. B., Ocheltree, T., Tissue, D. T., … Wingate, L. (2015). Optimal stomatal behaviour around the world. *Nature Climate Change*, *5*(5), 459–464. https://doi.org/10.1038/nclimate2550

Lombardozzi, D. L., Bonan, G. B., Smith, N. G., Dukes, J. S., & Fisher, R. A. (2015). Temperature acclimation of photosynthesis and respiration: A key uncertainty in the carbon cycle-climate feedback. *Geophysical Research Letters*, *42*, 8624–8630.

Ma, X. L., Huete, A., Moore, C. E., Cleverly, J., Hutley, L. B., Beringer, J., Leng, S., Xie, Z. Y., Yu, Q., & Eamus, D. (2020). Spatiotemporal partitioning of savanna plant functional type productivity along NATT. *Remote Sensing of Environment*, *246*, 111855. https://doi.org/10.1016/j.rse.2020.111855

Macinnis-Ng, C., Zeppel, M., Williams, M., & Eamus, D. (2011). Applying a SPA model to examine the impact of climate change on GPP of open woodlands and the potential for woody thickening. *Ecohydrology*, *4*(3), 379–393. https://doi.org/10.1002/eco.138

Mau, A. C., Reed, S. C., Wood, T. E., & Cavaleri, M. A. (2018). Temperate and tropical forest canopies are already functioning beyond their thermal thresholds for photosynthesis. *Forests*, 9(1), 47. https://doi.org/10.3390/f9010047

Medlyn, B. E., Dreyer, E., Ellsworth, D., Forstreuter, M., Harley, P. C., Kirschbaum, M. U. F., Le Roux, X., Montpied, P., Strassemeyer, J., Walcroft, A., Wang, K., & Loustau, D. (2002). Temperature response of parameters of a biochemically based model of photosynthesis. II. A review of experimental data. *Plant Cell and Environment*, 25(9), 1167–1179. https://doi.org/10.1046/j.1365-3040.2002.00891.x

Medlyn, B. E., Duursma, R. A., Eamus, D., Ellsworth, D. S., Prentice, I. C., Barton, C. V. M., Crous, K. Y., de Angelis, P., Freeman, M., & Wingate, L. (2011). Reconciling the optimal and empirical approaches to modelling stomatal conductance. *Global Change Biology*, 17(6), 2134–2144. https://doi.org/10.1111/j.1365-2486.2010.02375.x

Mercado, L. M., Medlyn, B. E., Huntingford, C., Oliver, R. J., Clark, D. B., Sitch, S., Zelazowski, P., Kattge, J., Harper, A. B., & Cox, P. M. (2018). Large sensitivity in land carbon storage due to geographical and temporal variation in the thermal response of photosynthetic capacity. *New Phytologist*, 218(4), 1462–1477. https://doi.org/10.1111/nph.15100

Mooney, H. A., Bjorkman, O., & Collatz, G. J. (1978). Photosynthetic acclimation to temperature in desert shrub, *Larrea-divaricata*. 1. Carbon-dioxide exchange characteristics of intact leaves. *Plant Physiology*, 61(3), 406–410. https://doi.org/10.1104/pp.61.3.406

Moore, C. E., Beringer, J., Evans, B., Hutley, L. B., McHugh, I., & Tapper, N. J. (2016). The contribution of trees and grasses to productivity of an Australian tropical savanna. *Biogeosciences*, 13(8), 2387–2403. https://doi.org/10.5194/bg-13-2387-2016

Norby, R. J., Warren, J. M., Iversen, C. M., Medlyn, B. E., & McMurtrie, R. E. (2010). CO_2 enhancement of forest productivity constrained by limited nitrogen availability. *Proceedings of the National Academy of Sciences of the United States of America*, 107(45), 19368–19373. https://doi.org/10.1073/pnas.1006463107

Pan, Y. D., Birdsey, R. A., Fang, J. Y., Houghton, R., Kauppi, P. E., Kurz, W. A., Phillips, O. L., Shvidenko, A., Lewis, S. L., Canadell, J. G., Ciais, P., Jackson, R. B., Pacala, S. W., McGuire, A. D., Piao, S. L., Rautiainen, A., Sitch, S., & Hayes, D. (2011). A large and persistent carbon sink in the world's forests. *Science*, 333(6045), 988–993. https://doi.org/10.1126/science.1201609

Pinkard, E., Wardlaw, T., Kriticos, D., Ireland, K., & Bruce, J. (2017). Climate change and pest risk in temperate *eucalypt* and *radiata* pine plantations: A review. *Australian Forestry*, 80(4), 228–241. https://doi.org/10.1080/00049158.2017.1359753

R Core Team. (2017). *R: A language and environment for statistical computing*. http://www.R-project.org/

Sage, R. F., & Kubien, D. S. (2007). The temperature response of C-3 and C-4 photosynthesis. *Plant Cell and Environment*, 30(9), 1086–1106. https://doi.org/10.1111/j.1365-3040.2007.01682.x

Scafaro, A. P., Xiang, S., Long, B. M., Bahar, N. H. A., Weerasinghe, L. K., Creek, D., Evans, J. R., Reich, P. B., & Atkin, O. K. (2017). Strong thermal acclimation of photosynthesis in tropical and temperate wet-forest tree species: The importance of altered rubisco content. *Global Change Biology*, 23(7), 2783–2800. https://doi.org/10.1111/gcb.13566

Sendall, K. M., Reich, P. B., Zhao, C. M., Hou, J. H., Wei, X. R., Stefanski, A., Rice, K., Rich, R. L., & Montgomery, R. A. (2015). Acclimation of photosynthetic temperature optima of temperate and boreal tree species in response to experimental forest warming. *Global Change Biology*, 21(3), 1342–1357. https://doi.org/10.1111/gcb.12781

Shinozaki, K., Yoda, K., Hozumi, K., & Kira, T. (1964). A quantitative analysis of plant form—The pipe model theory. I. Basic analyses. *Japanese Journal of Ecology*, 14(3), 97–104.

Sitch, S., Huntingford, C., Gedney, N., Levy, P. E., Lomas, M., Piao, S. L., Betts, R., Ciais, P., Cox, P., Friedlingstein, P., Jones, C. D., Prentice, I. C., & Woodward, F. I. (2008). Evaluation of the terrestrial carbon cycle, future plant geography and climate-carbon cycle feedbacks using five dynamic global vegetation models (DGVMs). *Global Change Biology*, 14(9), 2015–2039. https://doi.org/10.1111/j.1365-2486.2008.01626.x

Slot, M., & Winter, K. (2017). Photosynthetic acclimation to warming in tropical forest tree seedlings. *Journal of Experimental Botany*, 68(9), 2275–2284. https://doi.org/10.1093/jxb/erx071

Smith, N. G., & Dukes, J. S. (2013). Plant respiration and photosynthesis in global-scale models: Incorporating acclimation to temperature and CO_2. *Global Change Biology*, 19(1), 45–63. https://doi.org/10.1111/j.1365-2486.2012.02797.x

Smith, N. G., & Dukes, J. S. (2017). Short-term acclimation to warmer temperatures accelerates leaf carbon exchange processes across plant types. *Global Change Biology*, 23(11), 4840–4853. https://doi.org/10.1111/gcb.13735

Smith, N. G., & Keenan, T. F. (2020). Mechanisms underlying leaf photosynthetic acclimation to warming and elevated CO_2 as inferred from least-cost optimality theory. *Global Change Biology*, 26(9), 5202–5216. https://doi.org/10.1111/gcb.15212

Smith, N. G., Lombardozzi, D., Tawfik, A., Bonan, G., & Dukes, J. S. (2017). Biophysical consequences of photosynthetic temperature acclimation for climate. *Journal of Advances in Modeling Earth Systems*, 9(1), 536–547. https://doi.org/10.1002/2016ms000732

Smith, N. G., Malyshev, S. L., Shevliakova, E., Kattge, J., & Dukes, J. S. (2016). Foliar temperature acclimation reduces simulated carbon sensitivity to climate. *Nature Climate Change*, 6, 407–411.

Smith, N. G., McNellis, R., & Dukes, J. S. (2020). No acclimation: Instantaneous responses to temperature maintain homeostatic photosynthetic rates under experimental warming across a precipitation gradient in *Ulmus americana*. *Aob Plants*, 12(4), plaa027. https://doi.org/10.1093/aobpla/plaa027

Stinziano, J. R., Bauerle, W. L., & Way, D. A. (2019). Modelled net carbon gain responses to climate change in boreal trees: Impacts of photosynthetic parameter selection and acclimation. *Global Change Biology*, 25(4), 1445–1465. https://doi.org/10.1111/gcb.14530

Stinziano, J. R., Way, D. A., & Bauerle, W. L. (2018). Improving models of photosynthetic thermal acclimation: Which parameters are most important and how many should be modified? *Global Change Biology*, 24(4), 1580–1598. https://doi.org/10.1111/gcb.13924

Sun, Y., Gu, L., Dickinson, R. E., Norby, R. J., Plallardy, S. G., & Hoffman, F. M. (2014). Impact of mesophyll diffusion on estimated global land CO_2 fertilisation. *Proceedings of the National Academy of Sciences of the United States of America*, 111(44), 15774–15779. https://doi.org/10.1073/pnas.1418075111

Taylor, K. E., Stouffer, R. J., & Meehl, G. A. (2012). An overview of CMIP5 and the experiment design. *Bulletin of the American Meteorological Society*, 93(4), 485–498. https://doi.org/10.1175/bams-d-11-00094.1

Teckentrup, L. (2023). *The future of terrestrial carbon in Australia*. The University of NSW.

van Vuuren, D. P., Edmonds, J., Kainuma, M., Riahi, K., Thomson, A., Hibbard, K., Hurtt, G. C., Kram, T., Krey, V., Lamarque, J.-F., Masui, T., Meinshausen, M., Nakicenovic, N., Smith, S. J., & Rose, S. K. (2011). The representative concentration pathways: An overview. *Climatic Change*, 109(1), 5–31. https://doi.org/10.1007/s10584-011-0148-z

Vico, G., Way, D. A., Hurry, V., & Manzoni, S. (2019). Can leaf net photosynthesis acclimate to rising and more variable temperatures? *Plant Cell and Environment*, 42(6), 1913–1928. https://doi.org/10.1111/pce.13525

Walker, A. P., Beckerman, A. P., Gu, L. H., Kattge, J., Cernusak, L. A., Domingues, T. F., Scales, J. C., Wohlfahrt, G., Wullschleger, S. D., & Woodward, F. I. (2014). The relationship of leaf photosynthetic traits—V_{cmax} and J_{max}—To leaf nitrogen, leaf phosphorus, and specific leaf area: A meta-analysis and modeling study. *Ecology and Evolution*, 4(16), 3218–3235. https://doi.org/10.1002/ece3.1173

Walker, A. P., De Kauwe, M. G., Bastos, A., Belmecheri, S., Georgiou, K., Keeling, R. F., McMahon, S. M., Medlyn, B. E., Moore, D. J. P., Norby, R. J., Zaehle, S., Anderson-Teixeira, K. J., Battipaglia, G., Brienen, R. J. W.,

Cabugao, K. G., Cailleret, M., Campbell, E., Canadell, J. G., Ciais, P., ... Zuidema, P. A. (2021). Integrating the evidence for a terrestrial carbon sink caused by increasing atmospheric CO_2. *New Phytologist*, *229*(5), 2413–2445. https://doi.org/10.1111/nph.16866

Wang, S. (2020). Recent global decline of CO_2 fertilization effects on vegetation photosynthesis. *Science*, *370*, 1295–1300.

Wang, Y. P., Law, R. M., & Pak, B. (2010). A global model of carbon, nitrogen and phosphorus cycles for the terrestrial biosphere. *Biogeosciences*, *7*(7), 2261–2282. https://doi.org/10.5194/bg-7-2261-2010

Wang, Y. P., & Leuning, R. (1998). A two-leaf model for canopy conductance, photosynthesis and partitioning of available energy I: Model description and comparison with a multi-layered model. *Agricultural and Forest Meteorology*, *91*(1–2), 89–111. https://doi.org/10.1016/s0168-1923(98)00061-6

Way, D. A., & Yamori, W. (2014). Thermal acclimation of photosynthesis: On the importance of adjusting our definitions and accounting for thermal acclimation of respiration. *Photosynthesis Research*, *119*(1–2), 89–100. https://doi.org/10.1007/s11120-013-9873-7

Wright, S. J., Muller-Landau, H. C., & Schipper, J. (2009). The future of tropical species on a warmer planet. *Conservation Biology*, *23*(6), 1418–1426. https://doi.org/10.1111/j.1523-1739.2009.01337.x

Yamori, W., Hikosaka, K., & Way, D. A. (2014). Temperature response of photosynthesis in C-3, C-4, and CAM plants: Temperature acclimation and temperature adaptation. *Photosynthesis Research*, *119*(1–2), 101–117. https://doi.org/10.1007/s11120-013-9874-6

SUPPORTING INFORMATION

Additional supporting information can be found online in the Supporting Information section at the end of this article.